ENGINEERING TOOLS TO PROMOTE AND CHARACTERIZE WNT-MEDIATED STEM CELL DIFFERENTIATION

A Dissertation
Presented to
The Academic Faculty

by

Mark Stathos

In Partial Fulfillment
of the Requirements for the Degree
Doctorate of Philosophy (Ph.D.) in the
Interdisciplinary Bioengineering Graduate Program

Georgia Institute of Technology
August 2021

ENGINEERING TOOLS TO PROMOTE AND CHARACTERIZE WNT-MEDIATED STEM CELL DIFFERENTIATION

Approved by:

Dr. Ravi S. Kane, Advisor
School of Chemical and Biomolecular Engineering
Georgia Institute of Technology

Dr. Ronghu Wu
School of Chemistry and Biochemistry
Georgia Institute of Technology

Dr. Andrés García
School of Mechanical Engineering
Georgia Institute of Technology

Dr. Todd Sulchek
School of Mechanical Engineering
Georgia Institute of Technology

Dr. Manu Platt
Department of Biomedical Engineering
Georgia Institute of Technology

Date Approved: July 15, 2021

To my parents, Gloria and Steven, for fostering in me a passion for science and engineering for as long as I can remember

ACKNOWLEDGEMENTS

First and foremost, I would like to thank my advisor, Dr. Ravi Kane, for his personal and professional mentorship for the past five years. His high standards, excellent communication skills, and depth and breadth of scientific knowledge are inspirational to me and he has helped me grow immensely as a scientist throughout my graduate career. I would also like to thank my thesis committee members Dr. Andrés García, Dr. Manu Platt, Dr. Todd Sulchek and Dr. Ronghu Wu for their expertise and feedback throughout my graduate career.

I would next like to thank Dr. Chad Varner and Dr. Abhirup Mukherjee for the extensive training they provided me. Without their contributions none of this work would have been possible.

I would also like to thank my colleagues from the Kane lab Dr. Neha Dhar, Dr. Jihun Park, Dr. Tania Rosen, Dr. Ammar Arsiwala, Dr. Ana Castro, Troy Batugal, Steven Frey, Nicole Hu, Geetanjali Pendyala, Nikki McArthur, and Kathryn Loeffler. I could not have asked for a finer group of people with whom to share a lab. I would also like to thank those who I had the privilege of mentoring Nikolai Peterson, Jordan Bethea, Alec Zhan, James Platt and Evelyn LaRose. I am very proud of all of them and their accomplishments. The opportunities to work with them were powerful motivators and catalysts for significant personal growth.

I would like to give special thanks to those who played pivotal roles in helping me decide my career path: Douglas White, my mentor at Takeda, who gave me valuable insight into what to expect from graduate school; the late Dr. Bob Nerem who offered me serendipitous advice during an impromptu encounter without which I likely would not have pursued a PhD; and Dr. Krish Roy for encouraging me to be bold and unwavering in my pursuit of future professional opportunities.

I would next like to thank my friends: Troy Batugal, Karen Martin, Hannah Viola, Kelly Leguineche, Dr. Mason Chilmonczyk, Austin Culberson, Dr. Vanessa Cox, Jenni Farrar, and Dr. Jamie Davey for easing the burden of a long and challenging endeavor.

I would like to thank the entire CMaT community for giving me more new opportunities, connections, and resources to help me grow as a scientist than I ever could have imagined.

I would like to thank the following faculty with whom I have collaborated over the course of my graduate career, Dr. David Schaffer, Dr. Andrei Federov, Dr. Corey Wilson, and Dr. Melissa Kemp as well as all of their students. I would also especially like to thank Dr. Palecek and his students Martha Floy, Aaron Simmons, and Gyuhyung Jin for hosting me during a training sabbatical at the University of Wisconsin Madison and for providing me with extensive advice regarding stem cells and cardiomyocytes.

I would like to thank Dr. Brandon Dixon and Dr. David MacNair for their guidance and mentorship during my teaching practicum and teaching assistantship.

I would like to thank core lab directors Aaron Lifland, Sommer Durham, Laxminarayanan Krishnan, Andrew Shaw, and Bettina Bommarius for their training, troubleshooting and valuable insight.

I would like to thank my girlfriend, Emma Moran, for her endless patience and unwavering support and for bringing a sense of balance to my graduate school experience.

Finally, I would like to thank my parents, Gloria and Steven, and my sister Stephanie for helping me develop the curiosity, persistence, and passion for science required to complete a PhD.

TABLE OF CONTENTS

LIST OF FIGURES

LIST OF SYMBOLS AND ABBREVIATIONS

$[B_0]$	Concentration of cytosolic β-catenin
$[B_1]$	Concentration of CK1-phosphorylated β-catenin
$[B_2]$	Concentration of GSK3-phosphorylated β-catenin
$[B_3]$	Concentration of ubiquitinylated β-catenin
ANOVA	Analysis of Variance
AP-1	Activator protein 1
APC	Adenomatous polyposis coli
ATCC	American type culture collection
BCA	Bicinchoninic acid
BMP4	Bone morphogenesis protein 4
BSA	Bovine Serum Albumin
CAR-T	Chimeric antigen receptor T cell
Cas9	CRISPR associated protein 9
CH1	first domain of the constant region of the human IgG heavy chain
CK1	Casein kinase 1
CK1-p-β-catenin	CK1-phosphorylated β-catenin
CL	Constant region of the human IgG kappa light chain
CL6mN	**C**ry2PHR-mCherry-**L**RP**6**c with **N** **m**utated PPPAP motifs
CMV	cytomegalovirus
COUP-TFII	chicken ovalbumin upstream promoter transcription factor 2
CO_2	Carbon dioxide
CRD	Cysteine rich domain

CRISPR	Clustered regularly interspersed short palindromic repeats
Cry2	Cryptochrome 2
CSL	CBF1, Suppressor of Hairless, Lag-1
Dkk	Dickkopf-related protein
DLS	Dynamic Light Scattering
DMEM	Dulbecco's modified eagle medium
DNA	Deoxyribonucleic acid
DPBS	Dulbecco's phosphate buffered saline
EDTA	Ethylenediaminetetraacetic acid
ELISA	enzyme-linked immunosorbent assay
FASP	Filter aided sample preparation
Fc	Fragment Crystallizable
Fzd	Frizzled
Fzd2	Frizzled 2
Fzd-Fc	Frizzled 2 cysteine-rich domain fused to a human IgG Fc region
GiWi	GSK3 inhibition Wnt inhibition
gRNA	Guide ribonucleic acid
GSK3	Glycogen synthase kinase 3
GSK3-p-β-catenin	GSK3-phosphorylated β-catenin
HDR	Homology directed repair
HEK	Human embryonic kidney
HIC	Hydrophobic interaction chromatography
HI-FBS	Heat-inactivated fetal bovine serum
HRP	Horseradish peroxidase
HSV-TK	Herpes Simplex Virus Thymidine Kinase

ICM	Inner cell mass
IEX	Ion exchange chromatgoraphy
igG	Immunoglobin G
iPSC	Induced pluripotent stem cell
IWP-2	Inhibitor of Wnt processing and secretion 2
k_1	Rate of phosphorylation of β-catenin by CK1
k_{-1}	Rate of dephosphorylation of CK1-p-β-catenin
k_2	Rate of phosphorylation of β-catenin by GSK3
k_{-2}	Rate of dephosphorylation of GSK3-p-β-catenin
k_3	Rate of ubiquitinylation of β-catenin by β-TrCP
k_{-3}	Rate of deubiquitinylation of β-catenin
k_{deg}	Rate of degradation of ubiquitinylated β-catenin
LC-MS/MS	Liquid Chromatography with Tandem Mass Spectrometry
LDS	lithium dodecyl sulfate
LGR	Leucine-rich repeat containing G protein-coupled receptors
LRP6	Low-density lipoprotein receptor related protein 6
LRP6-Fc	LRP6 ectodomain fused to a human IgG Fc region
MCS	Multiple cloning site
MESP1	Mesoderm Posterior basic helix-loop-helix Transcription Factor 1
MWCO	molecular weight cutoff
NHEJ	Nonhomologous end joining
NHS	N-hydroxysuccinimide
Ni-NTA	nickle-nitrilotriacetic acid
ODE	Ordinary differential equation
PBST	PBS containing 0.05% Tween-20

PCR	Polymerase chain reaction
PHR	Photolyase homology region
RMS	Root mean squared
ROCK	Rho associate protein kinase
ROCKi	ROCK inhibitor
RPA	Replication protein A
RPMI/B-27	Roswell Park Memorial Institute with B-27 supplement
S	Rate of synthesis of β-catenin
SDS-PAGE	sodium dodecyl sulfate polyacrylamide gel electrophoresis
SEC	Size exclusion chromatography
SFRP	Secreted frizzled-related proteins
TALENS	transcription activator-like effector nucleases
TAZ	Transcriptional coactivator with PDZ-binding motif
TBS	Tris buffered saline
TBST	Tris buffered saline containing 0.1% Tween-20
TCF	T cell factor
TMB	Tetramethylbenzidine
WIF	Wnt inhibitory factor
XIC	extracted ion current
YAP	Yes-associated protein
ZFN	Zinc finger nuclease
ZNRF	Zinc and ring finger proteins
β-TrCP	Beta-transducin repeat containing protein

SUMMARY

The Wnt signaling pathway plays an important role in the development of many tissues in the body, notably cardiac tissue, from the very earliest stage of the process. However, the precise mechanisms of the Wnt pathway and the specific roles it has in development in the context of different tissue types remain poorly understood. This is in part due to the complexity of embryonic development and in part due to the hydrophobicity of Wnt ligands which renders them expensive and difficult to purify in a usable form.

To overcome issues associated with the use of natural Wnt ligands, we have developed a heterodimer of Fabs which bind to the Wnt co-receptors LRP6 and Frizzled. We have demonstrated that this dimer can activate Wnt signaling with an efficacy comparable to that of the natural ligand.

To elucidate the mechanisms of downstream events in the Wnt pathway, we constructed a kinetic model consisting of a system of ordinary differential equations. We fit this model to empirical time course data derived from Western blots of HEK293T cells treated with Wnt. From this fit we were able to gain insights into how the intracellular levels of the Wnt pathway component β-catenin are regulated.

To better characterize the downstream effects of Wnt signaling during the manufacturing of therapeutic cells, we are also generating CRISPR/Cas9 edited reporter iPSC lines which will be able to detect the expression of Wnt-regulated marker genes such as Brachyury and COUP-TFII with high specificity. Luminescent signals produced

with the help of luciferase secreted by these cell lines during directed differentiation into cardiomyocytes permit continuous non-destructive monitoring of the manufacturing process. We have also employed a transcription amplification scheme to enhance these signals and ensure they are easily detectable in genome edited cell lines. These cell lines could potentially guide process optimization and enable production of cardiomyocytes with a more mature phenotype. These cells will also be equipped with an inducible suicide mechanism to enable their easy and selective removal during cell manufacturing applications involving co-culture with unedited cells.

CHAPTER 1. INTRODUCTION

1.1 Description of the Wnt Signaling Pathway

Wnt signaling plays an important role in a wide variety of physiological processes such as cell proliferation and cell migration. Mutations to Wnt signaling pathways have been implicated in several diseases including Alzheimer's, type II diabetes, and a variety of cancers.[1] However, Wnt signaling is perhaps most notable for its role embryogenesis.[2] Protocols involving modulating Wnt pathways have been used to generate several cell types with potential therapeutic applications including neurons[3] and cardiomyocytes[4] both of which have very limited capacity to regenerate in adults.

To create these cell types, Wnt, along with other signaling pathways, acts on stem cells. Stem cells are cells which have the potential to transform into one or more other cell types. This transformation process is called differentiation and the number of cell types a stem cell can become is known as potency. Stem cells derived from the earliest phases of embryonic development are totipotent meaning they can become any other cell type. However, most stem cell lines are derived from a slightly more mature embryonic developmental phase known as the blastocyst.[5] The blastocyst is comprised of a spherical inner cell mass surrounded by a protective outer layer. The outer layer eventually develops into placental and umbilical cord tissue while the inner cell mass, which is said to be pluripotent, can develop into any adult tissue type.[5] However, there are ethical concerns with using embryonic stem cells because the process of acquiring them results in the termination of the embryo.[5] To circumvent these issues, Takahashi et al. used a retroviral system to induce expression of the four genes Oct4, Sox2, Klf-4, and c-Myc to

reprogram adult human fibroblasts into stem cells which were pluripotent.[6] These cells were termed induced pluripotent stem cells (iPSCs). The impact of this discovery was monumental. This level of potency is sufficient for the generation of a wide variety of therapeutic cell types. Additionally, it made it possible to treat patients with autologous cells to avoid complications caused by induction of an immune response to foreign tissues. Refining differentiation protocols to generate high quality somatic cells of many types is a very active area of research. Attaining a better understanding of the signaling pathways involved in stem cell differentiation, such as Wnt, could therefore be vital for developing cell therapies for currently incurable conditions such as neurodegenerative diseases or cardiovascular disease.

However, despite the importance of Wnt signaling to regenerative medicine, many aspects of the pathway remain incompletely understood. For example, the structure of the signalosome has yet to be fully determined, the precise mechanism by which Wnt pathway component β-catenin translocates to the nucleus to initiate transcription remains unclear,[7] and it is not completely understood how Wnt is secreted and delivered to recipient cells.[8] A major impediment to detailed investigations is the fact that Wnt ligands are expensive to purchase from commercial sources and laborious to purify in an academic setting. Wnt is very hydrophobic due to several post-translational acylation additions. These modifications cannot be removed because they are critical for receptor binding[9] and they make the purification of Wnt ligands challenging. A purification protocol by Willert et al. details the addition of detergent followed by hydrophobic interaction chromatography, size exclusion chromatography, and ion exchange

chromatography but results in relatively low yield and the possibility of protein precipitation.[10]

While many details of the Wnt pathway have yet to be fully elucidated in part due to the aforementioned difficulties associated with the expression and purification of Wnt ligands, much has been determined in the thirty five years since the discovery of Wnt.

After transcription and translation, Wnts are modified with several glycosylations and a large lipidation in the form of a palmitoleic acid moiety. This lipidation is performed by the enzyme Porcupine in the endoplasmic reticulum. Lipidated Wnt then moves to the Golgi apparatus where it associates with the protein Wntless and is

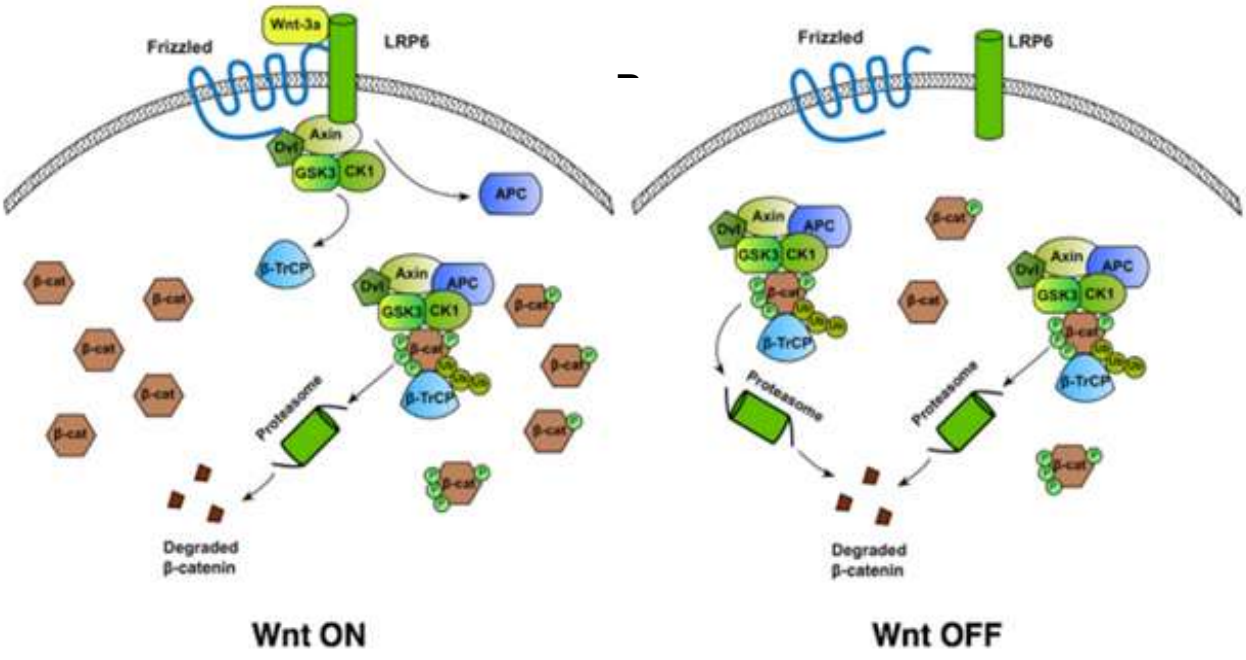

Figure 1. The Wnt Pathway Cascade in the Presence and Absence of Wnt A) When Wnt is bound to its receptors the destruction complex is pulled to the membrane and inactivated. B) When Wnt is absent, the destruction complex is located in the cytosol and destroys β-catenin. (Figure taken from Mukherjee et al.)[14]

secreted.[11] It has not been established how Wnt is transported to target cells once secreted but it is thought that it may be moved via exosomes.

Once Wnt reaches the target cells, it then binds to the cysteine rich domain (CRD) of its main receptor Frizzled (Fzd) burying its hydrophobic palmitoleic acid moiety into a groove in the receptor. Wnt also simultaneously engages Fzd at a secondary site on the opposite side of the Fzd CRD. Once Wnt has bound to Fzd, it then engages its secondary receptor Low-density lipoprotein receptor-related protein 6 (LRP6) most likely via a linker region between the "thumb" and "index finger" projections which bind to Fzd.[9] From here, Fzd and LRP6 homodimerize and form some type of higher order structure.[12] The extent of signaling can be modulated by other ligands such as sclerostin or Dkks (Dickkopf-related proteins) which bind to LRP6 to inhibit signaling, Wnt inhibitory factors (WIFs) and Secreted Frizzled-Related Proteins (SFRPs) which sequester Wnt, or R-spondin which binds to receptors Leucine-rich repeat containing G protein-coupled receptors (LGRs) and Zinc and ring finger proteins (ZNRFs) and prevents endocytosis and degradation of Wnt receptors to augment Wnt-induced signaling.

Once the signalosome has been assembled, intracellular signaling is initiated as shown in Figure 1A. Disheveled is recruited to the intracellular C-terminus of Fzd and the intracellular portion of LRP6 becomes phosphorylated by Casein kinase 1γ (CK1γ).[13] A portion of the β-catenin destruction complexes then translocate to the membrane, and the resulting disassembly of these destruction complexes in which adenomatous polyposis coli (APC) dissociates from the rest of the complex results in a reduction in the rate of degradation of the transcriptional co-activator, β-catenin.[14] This reduction leads to the accumulation β-catenin in the cytosol and increased nuclear translocation. Nuclear β-

catenin then binds to the transcription factor T cell factor (TCF) changing it from a transcriptional repressor to an activator allowing increased expression of Wnt target genes.[15]

In contrast, in the absence of Wnt, (Figure 1B) the β-catenin destruction complex is located in the cytosol and actively tags β-catenin for degradation by phosphorylating it via Casein Kinase 1 (CK1), further phosphorylating it via Glycogen Synthase Kinase 3 (GSK3), and ubiquitinating it via beta-transducin repeat containing protein (β-TrCP). Ubiquitinated β-catenin is then degraded by the proteasome. This prevents most β-catenin from localizing to the nucleus and Wnt-regulated genes remain repressed.

1.2 The Role of Wnt in Cardiomyocyte Formation

Understanding how cell signaling regulates stem cell differentiation is critical for generating high quality cells of many types for academic and therapeutic applications. Differentiation into cardiomyocytes is of particular interest because it would address a major unmet clinical need. Many protocols for generating cardiomyocytes from stem cells have been developed and most of these involve modulating the Wnt pathway and/or the closely related activin A and bone morphogenesis protein 4 (BMP4) pathways. It is important to have a thorough understanding of the underlying mechanisms at play if one is to troubleshoot or improve upon these protocols. To that end we will now discuss the role of Wnt in cardiogenesis.

Wnt ligand expression was shown to be induced by activin A/BMP4 signaling in stem cells during the earliest phase of differentiation into mesodermal tissue[16] In turn, Wnt signaling was also shown to result in the phosphorylation and activation of Smad1,

the downstream effector of BMP4.[16] Brachyury, the principle driver of primitive streak formation and a marker of mesodermal tissue, is expressed as a direct result of this activin A/BMP4-induced Wnt signaling.[17] This initial Wnt signaling starts a feedback loop in which Wnt signaling upregulates expression of canonical Wnt inhibitors Wnt11 (a non-canonical Wnt) and Dkk1.[17] Once mesodermal tissue has formed, Wnt signaling and activin A/BMP4 signaling form orthogonal gradients along the anterior-posterior and dorsal-ventral axes of the developing embryo respectively. The region with low Wnt signaling and high activin A/BMP4 signaling eventually becomes cardiac tissue while regions of high Wnt signaling and low activin A/BMP4 signaling become vascular endothelial tissue.[18] Thus Wnt signaling has a biphasic effect on cardiomyocyte differentiation. Wnt must be active to drive differentiation into mesoderm tissue but must later be inhibited to continue differentiation into cardiac tissue. Wnt signaling works with activin A/BMP4 signaling to generate cardiac tissue or vascular endothelium[19]

1.3 Reporter Genes and Biosensors to Study Development

In order to better understand signaling pathways such as Wnt or to quantify their activity over time, several so-called reporter genes are often employed. These generally include a wide variety of fluorescent proteins, oxidative enzymes such as luciferases which catalyze chemical reactions that result in the production of light, or other enzymes such as β-galactosidase which can catalyze the hydrolysis of a substrate, producing a color change.

One common use of these reporter genes is to place them downstream of a promoter of a target gene in a plasmid so that when the target gene is expressed the

reporter will be as well. Similarly, by including several appropriately spaced transcription factor binding deoxyribonucleic acid (DNA) sequences upstream of a minimal promoter and a reporter gene, the extent of activation of particular signaling pathways can be measured. Yet another approach is to transfect cells with DNA encoding fusion proteins consisting of a target protein connected to a reporter protein by a flexible linker sequence.[20]

Generally, enzymes are used to study signaling pathway or promoter activity. This is because one enzyme molecule can rapidly catalyze the reaction of a large number of substrate molecules, thereby producing a strong signal even when present at low concentrations. Fluorescent proteins can be used in this way as well but generally offer lower sensitivity. Fluorescent proteins are more commonly used as fusions to the target protein to enable easy visualization. These markers can also be used for cell sorting if desired.

These reporter systems are often used in short-term transient transfection experiments. However, they can also be incorporated into the genome via viral transduction,[21] site specific recombination,[22] or by genome editing using clustered regularly interspaced short palindromic repeats (CRISPR) and CRISPR associated protein 9 (Cas9).[23] This approach is more time-consuming but allows the creation of stable cell lines (or even animal models)[22] which produce a more consistent signal without the need for repeated transfections.[24] This approach can also be used for longer term experiments such those involving stem cell differentiation.[25]

1.4 Suicide Genes

The advent of cell-based therapy such as chimeric antigen receptor T-cell (CAR-T) drugs has increased the need for inducible cellular suicide mechanisms. While these therapies are incredibly promising and have already been used clinically[26], there have been reports of severe side effects such a cytokine storm.[27] Furthermore, genome edited cells could potentially behave in unexpected ways *in vivo*. With conventional small molecule drug treatments or biologics, dosing can often simply be halted if severe side effects occur. However, this is not possible when the treatment is in the form of living cells. Instead, it is necessary to actively kill the engineered cells to mitigate side effects. Methods of accomplishing this rapidly, completely, and with minimal harm to other cell types are therefore of great interest to the field. This has primarily been accomplished by engineering cells to express genes that initiate apoptosis in response to small molecules which do not affect wild type cells.

1.5 Challenges and Specific Aims

Understanding and controlling Wnt signaling could have a significant impact on the treatment of a variety of diseases and greatly accelerate progress in regenerative medicine. However, despite its importance, there are several obstacles to controlling the Wnt pathway.

1.5.1 Wnt Ligands are Difficult and Expensive to Purify

Wnt ligands undergo many post-translational modifications including the addition of a palmitoleic acid motif. This modification is essential for Wnt binding to its target receptor but renders Wnt very hydrophobic and poorly soluble in aqueous solutions.

1.5.2 Mechanisms of the Intracellular Events of the Wnt Pathway Remain Poorly Understood

The specific molecular mechanisms that govern the processing and degradation of the Wnt pathway component β-catenin remain controversial. It is unclear which steps in this process are most affected by Wnt ligands. This hampers our understanding of the pathway as well as the development of drugs targeting the pathway.

1.5.3 It is Difficult to Understand Downstream Effects of Wnt Signaling

Wnt signaling is critical for embryonic development and stem cell differentiation but producing well-characterized high quality cell products from stem cells remains challenging. This is largely due to the complex network of genes whose expression depends directly or indirectly on activation of the Wnt pathway.

In this work, we have attempted to address the aforementioned challenges in a variety of ways. Our overall goal was to develop tools to activate and help further understand and characterize the Wnt pathway.

1.5.4 Specific Aim 1: Developing a Synthetic Wnt Agonist

1.5.5 Specific Aim 2: Modelling the Wnt Pathway

1.5.6 Specific Aim 3: Developing Reporters to Track iPSC Differentiation into Cardiomyocytes

CHAPTER 2. DEVELOPING A SYNTHETIC AGONIST OF THE CANONICAL WNT SIGNALING PATHWAY[1,2]

2.1 Introduction

The canonical Wnt signaling pathway plays a key role in the embryonic development of virtually all animal species. This pathway has also been directly implicated in a variety of cancers and some pathway components have been implicated in other pathologies such as type II diabetes and Alzheimer's disease.[29] However, research in this area is hampered by the expense and difficulty associated with purifying active Wnt ligands. This is due to the presence of a post-translational modification – the addition of a palmitoleic acid moiety which is essential for binding to Fzd receptors but which also renders Wnt ligands insoluble in aqueous solution.[9, 30]

Consequently, there has been much interest in circumventing these issues by developing alternative methods to activate the Wnt pathway. The first method to be developed was the treatment of cells with Li^+. This treatment prevents the degradation of β-catenin by inhibiting the activity of GSK3.[31] However, Li^+ also interferes with the activity of several other cellular proteins such as G-protein coupled receptors, a variety of phosphatases, and the transcription factor activator protein 1 (AP-1).[32] Thus, it is not a specific activator of Wnt signaling. A more recently developed alternative is the small

[1] Western blot and activation dose response were performed by my colleague Dr. Abhirup Mukherjee. Mass spectroscopy was performed by Dr. David Smalley

[2] This chapter is based on our work published in ChemComm:

28. Mukherjee, A.; Stathos, M. E.; Varner, C.; Arsiwala, A.; Frey, S.; Hu, Y.; Smalley, D. M.; Schaffer, D. V.; Kane, R. S., One-pot synthesis of heterodimeric agonists that activate the canonical Wnt signaling pathway. *Chemical Communications* **2020,** *56* (25), 3685-3688.

molecule CHIR99021, which also targets GSK3 but with much greater specificity.[31] However, CHIR99021 activates signaling through a different mechanism than that the natural Wnt ligand which causes partial inactivation of CK1 and β-TrCP in addition to GSK3.[33] Furthermore, GSK3 phosphorylates many other target proteins in addition to β-catenin and plays a role in other pathways such as insulin signaling; thus, directly inhibiting its activity may lead to undesired side effects.[34]

Cong et al. showed that heterodimerization of Fzd and LRP6 is sufficient to activate Wnt signaling.[35] Using this development, Janda et al. generated synthetic dimers which simultaneously bind to Fzd and LRP6 and are capable of activating Wnt signaling *in vitro* and *in vivo*.[36] This was a major advancement in the development of Wnt alternatives. However, the fusion consisted in part of the natural ligand Dkk which binds to LRP6. Natural ligands are not necessarily amenable to fusion with other proteins, may not have high expression yield, and lack tunability in binding site and affinity which means a similar design may not be suitable for other applications requiring receptor heterodimerization.

To address these issues we developed a protein-based synthetic Wnt activator using an approach that could more easily be generalized to other applications of heterodimerization such as activating G-protein coupled receptors or engaging T cells.[28] Specifically, we expressed modified human anti-Fzd and anti-LRP6 antigen binding fragments (Fabs) and linked them together using SpyCatcher-SpyTag chemistry.[37] SpyCatcher and SpyTag are a protein-peptide pair isolated from a bacterial adhesin which interact to form a covalent bond. The resulting Fab heterodimer was shown to activate

Wnt signaling in Human Embryonic Kidney 293 T cells (HEK293T) cells comparably to commercial Wnt-3a (Fig. 2).

2.2 Design Considerations for Heterodimer and Other Multivalent Ligands

Linker length, linker composition, and valency are critical parameters governing the potency of engineered multivalent proteins such as our heterodimer. Linkers comprised of glycine and serine repeats are widely used because their flexibility facilitates multivalent binding. To that end, we chose to use repeats of GGGGS for our linkers. Janda et al. characterized a variety of lengths of flexible linkers between the Fzd- and LRP6- binding portions of their engineered Wnt agonist.[38] They found that signaling was activated for all lengths between 0 and 15 amino acids, suggesting that a wide range of linker lengths are suitable for this application. Because a linker of insufficient length may not allow binding to both receptors simultaneously, whereas an overly long linker is likely to only result in a modest increase in binding affinity, we constructed a linker at the higher end of (but still within) the range identified by Janda et al.[38] In general, when designing a multivalent ligand, it is best to determine the desired spacing using available crystal structures when possible and then design constructs with flexible linkers consisting of repeats of GGGGS or a similar sequence such that the estimated root mean squared (RMS) end-to-end distance for the linker is equal to or larger than the desired spacing between the ligands being connected.[39] From this starting point, variations in linker length can be explored until an optimal length is determined. Generally, higher valency also results in increased avidity.

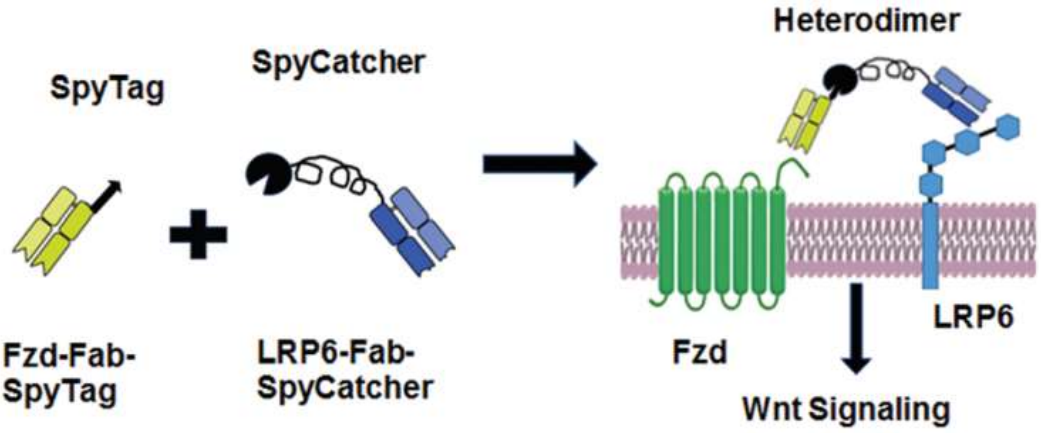

Figure 2 Schematic of a heterodimer agonist binding to the membrane proteins Frizzled and LRP6. Fusing Frizzled (Fzd) and LRP6 Fabs via SpyCatcher–SpyTag interaction forms a heterodimer that binds to the canonical Wnt pathway receptors Fzd and LRP6. Reproduced from Mukherjee et al.[28] with permission from the Royal Society of Chemistry

2.3 Material and Methods

2.3.1 Plasmid Construction

The 7x TCF Wnt luciferase reporter[21] was constructed with a pVitro2-MCS vector with a hygromycin resistance gene for bacterial transformation (Invivogen). In the first cloning site (MCS-1), the ferritin promoter and cytomegalovirus (CMV) enhancer were removed and replaced with 7 repeats of the consensus TCF binding sequence followed by a minimal promoter (minP) and subsequently the firefly luciferase gene. Gene synthesis and cloning were performed by Gene Universal. The anti-Fzd Fab and anti-LRP6 Fab were engineered from Frizzled antibody and LRP6 antibody sequences obtained from patents by Gurney et al. and Jenkins et al. respectively.[40] The expression plasmids were constructed by inserting the variable regions of the light chain and heavy chain sequences into the TGEX-LC and TGEX-FH vectors (Antibody Design Labs). The TGEX vectors code for the first domain of the constant region of the human

immunoglobin G (IgG) heavy chain (CH1) with a C-terminal 6x His tag and the constant region of the human kappa light chain (CL). One repeat of a GGGGS linker sequence followed by the SpyTag sequence was inserted between the CH1 region and the C-terminal 6x His tag of the heavy chain of the anti-Fzd Fab. The SpyCatcher sequence was inserted at the C-terminus of LRP6 following a GGGGSKLGDIEFIKVNKGGGGS linker sequence. All plasmids were custom-synthesized and cloned into the TGEX vector by Gene Universal.

2.3.2 Expression of Recombinant Antibody Fragments

Forty five mL of HEK293F (Thermo Scientific) mammalian cells suspended in Expi293 Expression Medium (Thermo Scientific) were grown up to a density of 2.9 million cells per mL in a 125-mL Erlenmeyer flask in a humidified incubator at 37 °C with 8% carbon dioxide (CO_2) concentration. Cultures for Fab expression were transfected with plasmids encoding the heavy chain and light chain in a 1:2 w/w ratio. Transfection was performed using the ExpiFectamine (Thermo Scientific) transfection reagent according to the manufacturer's recommendation. Recommended doses of transfection enhancers were added to the culture 20-24 hours after initial addition of transfection reagents. Post transfection, cells were incubated for 6 days and then pelleted. The Expi293F (Thermo Scientific) supernatant media was harvested to proceed with purification of the Fabs.

2.3.3 ELISAs

For enzyme linked immunosorbent assays (ELISAs), commercial LRP6 ectodomain fused to a human IgG crystallizable fragment (Fc) region (LRP6-Fc) (R&D

Systems) and Frizzled 2 (Fzd2) cysteine-rich domain (CRD) fused to a human IgG Fc region (Fzd-Fc) (R&D Systems) were diluted in carbonate buffer (pH 9.6) to a concentration of 1 μg/mL. The antigens were used to coat a Maxisorp 96-well plate (Thermo Scientific) overnight at 4°C. Fabs were biotinylated with SulfoEZ-link N-hydroxysuccinimide (NHS) Biotin (Thermo Scientific) with a 50x molar excess of biotin at 4°C overnight. The next day, each well was blocked using 5% bovine serum albumin (BSA) solution in phosphate buffered saline containing 0.05% Tween-20 (PBST) for 1 hour at room temperature. The blocked wells were then incubated with the respective Fabs diluted to a concentration of 2 μg/mL in PBST with 1% BSA and then with the respective secondary anti-human antibody (Jackson Immunoresearch) or streptavidin (Thermo Scientific) horseradish peroxidase (HRP) conjugates diluted in 1% BSA solution in PBST at a concentration recommended by the manufacturer. All wells were washed thoroughly with 200 μL of PBST in between incubation steps. Finally, the wells were incubated with 100 μL 3,3′,5,5′-Tetramethylbenzidine (TMB) (Thermo Scientific) solution for 15 minutes followed by the addition of 100 μL of 0.16 M sulfuric acid. Next, the absorbance at 450 nm was read using a BioTek Synergy plate reader.

2.3.4 Purification of Dimer

The Expi media was dialyzed into 1x PBS twice for two hours to remove Ethylenediaminetetraacetic acid (EDTA) present in the media which would interfere with purification. The supernatant containing unreacted Fzd-Fab-SpyTag, LRP6-Fab-SpyCatcher and the Fzd-Fab-LRP6-Fab heterodimers was then purified using 1 mL nickle-nitrilotriacetic acid (Ni-NTA) (Thermo Scientific) agarose resin with specific affinity for the His tag in 30 mL columns at 4 °C. Each Ni-NTA column was first

equilibrated with 20 column volumes of equilibration buffer (50 mM Tris, 500 mM NaCl, 25 mM imidazole, 5% glycerol, pH 8.0). The supernatant was then passed through the column and the flow through discarded. The column was then washed using 50 mM imidazole buffer (pH 8.0) once to get rid of non-specific protein binding in the resin and the flow through was collected. The protein of interest was then eluted with 400 mM imidazole (pH 8.0) buffer in 2 mL fractions and all the fractions were collected. The eluted proteins were then concentrated down to less than 1 mL by centrifuging at 4500x g in Amicon 10kDa molecular weight cutoff (MWCO) 15 mL spin filters (EMD Millipore). The 1 mL eluate was then purified in a HiLoad Superdex 200 column in the case of the heterodimer or a Superdex 75 column in the case of individual Fabs loaded on an ÄKTA Pure chromatography system (GE Healthcare) using size-exclusion chromatography at 4 °C. The fractions corresponding to the peaks in absorbance at 280 nm were run on a sodium dodecyl sulfate polyacrylamide gel electrophoresis (SDS-PAGE) gel and analyzed for purity using Coomassie Brilliant Blue Staining (Thermo Scientific). Fractions containing dimers were pooled and concentrated again in an Amicon 10kDa MWCO 15 mL spin filter. The purified proteins were then aliquoted and stored. For short-term use, purified heterodimers were stored in PBS containing >40% glycerol at -20°C. For long-term storage, purified fractions were frozen in -80°C in PBS containing >40% glycerol.

2.3.5 Luciferase Assays for Activation and Inhibition

HEK293T cells (CRL-11268) were purchased from American type culture collection (ATCC) and cultured in Dulbecco's modified eagle medium (DMEM) (high-glucose) supplemented with 10% Fetal Bovine Serum (FBS) (Gibco, Thermo Scientific)

in a humidified incubator at 37 °C with 8% CO_2 concentration. HEK293T cells were plated on a 6-well plate coated with poly-L-lysine and grown up to 80% confluency. The cells were then transfected with the 7x TCF reporter plasmid, trypsinized 24 hours after transfection (0.25% Trypsin-EDTA, Thermo Scientific), re-plated in a 96-well plate (Corning) coated with poly-L-lysine (SigmaAldrich). Transfected cells were then treated with different concentrations of heterodimers, Wnt-3a, or Fabs diluted in 1x DMEM media (Gibco) with 10% FBS (Gibco) as appropriate. Each treatment was done in triplicate. After 24 hours of treatment, cells were lysed in a passive lysis buffer (Promega) and centrifuged in the 96-well plate (Corning) at 2000×g for 10 minutes to remove debris from the cell lysate. The cleared cell lysates were then transferred to an opaque white 96-well plate (Corning). Luminescence signal was then measured from each well in a BioTek Synergy plate reader immediately following the addition of the Luciferase Assay Reagent (Promega).

2.3.6 Western Blot

HEK293T cells were cultured in 6-well tissue culture plates (Corning) and grown up to 90% confluency. After treatment, the cells were washed in ice-cold Dulbecco's phosphate buffered saline (DPBS) (Corning) twice and 80 µL of lysis buffer, consisting of 0.5% (w/v) digitonin (pH 7.5) in DPBS, was added to each well. The lysis buffer was supplemented with N-ethylmaleimide (Sigma-Aldrich) at a concentration of 5 µM and phosphatase inhibitor (Sigma-Aldrich) and protease inhibitor cocktails (Thermo Scientific) at dilutions recommended by the manufacturer. The lysates were incubated on ice for 30-45 minutes for complete lysis and harvested using cell scrapers (Grainger). The lysates were then cleared by centrifuging at 13,000×g for 15 minutes. The clear, debris-

free supernatant was collected for further analysis for each lysate. These represented the whole-cell lysates. Because most cellular β-catenin is bound to the cell membrane and does not participate in Wnt signaling, we next obtained the cytoplasmic and nuclear extract by incubating the supernatant with Concanavalin A-Sepharose 4B beads (GE Healthcare) for 60 minutes at 4°C with continuous end-over-end mixing. The slurry was then centrifuged at 4000×g for 5 minutes. The membrane-associated proteins were bound to the Concanavalin A beads and the supernatant consisted of the cytoplasmic and nuclear fractions of the lysate. The beads were then washed 5 times with DPBS and denatured directly in 2x lithium dodecyl sulfate (LDS) Sampling Buffer (Thermo Scientific). Lysates were then resolved using SDS-PAGE in 3-8% Tris-Acetate gels using an OWL P8DS (Thermo Scientific) gel-running apparatus. The proteins were then transferred using the Trans-Blot Turbo Transfer System (Bio-Rad) to a 0.2 μm pore size nitrocellulose membrane. For immunoblotting, the membrane was blocked in a blocking buffer (1x Tris buffered saline (TBS) with 0.1% Tween-20 and 5% non-fat dry milk or BSA; as per antibody manufacturer's recommendation) for 1 hour at room temperature. The membrane was then incubated overnight at 4°C in primary antibody diluted in 5% BSA in TBST (1x TBS containing 0.1% Tween-20). The dilution used for the primary anti-β-catenin and anti-vinculin antibodies was 1:1000. Next, the membrane was washed three times with TBST for 5 minutes each and then incubated in secondary antibody diluted in the blocking buffer for 1 hour at room temperature with constant mixing. An HRP-conjugated anti-mouse antibody (Jackson Immunoresearch) was used to detect total β-catenin at a dilution of 1:10000. Vinculin was detected using an HRP conjugated anti-rabbit antibody (Thermo Scientific) at a dilution of 1:3000. The membrane was then

imaged in a ChemiDoc MP Imaging system (Bio-Rad) after 1 minute of incubation in the SuperSignal West Femto Maximum Sensitivity Substrate. The detected protein bands were quantified using the analysis tools provided in the Image Lab Software (Bio-Rad) and then validated using ImageJ.

2.3.7 Protein Quantitation by BCA Assay

The bicinchoninic acid (BCA) assay was performed using a kit purchased from Pierce using manufacturer's instructions. In brief, the supplied 2.0 mg/mL BSA standard was serially diluted two-fold in PBS. Next, 25 µL of each sample or standard were pipetted into the wells of a 96- well plate. The provided cupric sulfate solution was then diluted into a provided solution containing BCA at a 1:50 volume ratio. A volume of 200 µL of this reagent was added to each well and the plate was covered with tape and incubated at 37 ºC for 30 minutes. The absorbance at 562 nm was read and a standard curve generated from the BSA dilutions. A linear regression was performed to relate concentration to absorbance and the concentration of the samples was determined by interpolation.

2.3.8 Sample Preparation, Trypsin Digestion, Liquid Chromatography with Tandem Mass Spectrometry (LC-MS/MS), and Peptide Identification

The proteins in each sample were reduced, alkylated and digested with trypsin according to the Filter aided sample preparation (FASP) protocol.[41] The peptides were analyzed by nano-LC-MS/MS, and peptide identification as previously described[42] with the following modifications. Reverse phase chromatography was performed using an in-house packed column (40 cm long X 75 µm ID X 360 OD, Dr. Maisch GmbH ReproSil-

Pur 120 C18-AQ 1.9 µm beads) and a 120 min. gradient. The Raw files were searched using the Mascot algorithm (ver. 2.5.1) against a protein database constructed by combining the sequences of the heavy chain of the Fzd-Fab-SpyTag and the light chain of the LRP6-Fab-SpyCatcher and a contaminant database (cRAP, downloaded 11-21-16 from http://www.thegpm.org) via Proteome Discoverer 2.1. Additional modifications including FSK, FSKR, and FSKRDEDGK, which correspond to expected tryptic digest peptides that may be covalently linked to the aspartic acid residue in the SpyTag, were used and a "no enzyme" search was performed allowing cleavage at any residue. Only peptide spectral matches with expectation value of less than 0.01 ("High Confidence") were used. No cross-linked peptides were identified but spectral count analysis suggested that native peptides associated with the expected cross-link site were diminished. To verify this, the extracted ion current (XIC) for FSK from SpyCatcher and IVMVDAYKPTK from SpyTag was examined and found to be greatly reduced (Fig. 3). Other peptides examined (e.g. VFPLAPSSK) generated spectral counts and XICs consistent in the heterodimer with what was observed for the monomeric proteins containing SpyCatcher and SpyTag suggesting that the primary structure was not altered except in the regions expected to be cross-linked by SpyTag-SpyCatcher Chemistry. Cyclobranch could be a useful resource for detecting similar branched peptides for other applications.[43]

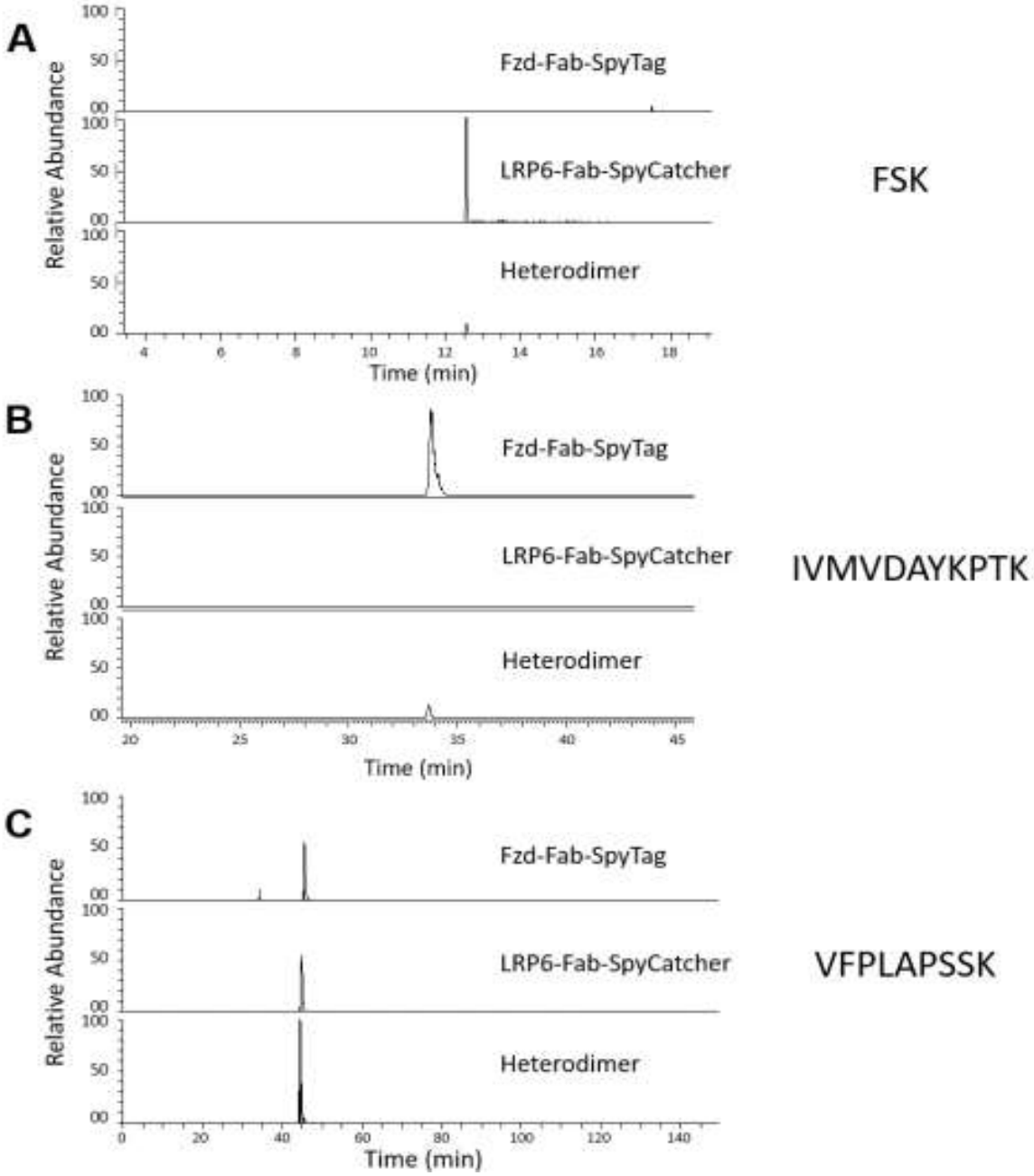

Figure 3 Characterization of Heterodimer Formation Reaction by LC-MS/MS. Extracted Ion Currents (XIC) for peptides from the tryptic digest of Fzd-Fab-SpyTag, LRP6-Fab-SpyCatcher, and Heterodimer for : A) FSK ([M+H]+), corresponding to a sequence in LRP6-FabSpyCatcher that is not expected to be detected in the Heterodimer after isopeptide bond formation; B) Peptide fragment IVMVDAYKPTK ([M+2H]+2), part of the SpyTag sequence that is not expected to be seen in the Heterodimer; and C) Peptide fragment VFPLAPSSK ([M+2H]+2), corresponding to a sequence that is present in both Fzd-Fab-SpyTag, and LRP6-Fab-SpyCatcher and heterodimer formation is not expected to alter its presence. Each set of chromatographs are on the same scale (1.0E6, 2.0E8, and 6.5E7, for A, B, and C, respectively) Reproduced from Mukherjee et al.[28] with permission from the Royal Society of Chemistry

2.3.9 Dynamic Light Scattering

Glycerol-free aliquots of 100 µL of purified protein at a concentration of at least 1 mg/mL were placed into cuvettes and inserted into a DynaPro NanoStar device from Wyatt Technologies. The chamber was warmed to 25 ºC and ten acquisitions were recorded for each sample. Data were reported using an isotropic sphere model.

2.3.10 Size Exclusion Chromatography Shifts

A sample of 5 µg of the purified heterodimer was run on a Superdex 200 gel filtration column (GE) immediately after cleaning with 0.5 M NaOH and equilibration in PBS at 4 °C. Absorbance at 210 nm was recorded. Next, additional runs were performed with LRP6-Fc (R&D Systems) and Fzd2-Fc (R&D Systems) alone. Finally, 5 µg of the heterodimer were mixed with at least a 2 fold excess of LRP6-Fc or Fzd2-Fc, incubated for 5 minutes at room temperature, and the mixture was run on the column at 4 °C.

2.3.11 SDS-PAGE

After purification, samples of proteins were taken and mixed with 4x NuPAGE lithium dodecyl sulfate sample buffer (Invitrogen) in a 3:1 volume ratio. Samples were then heated to 95 ºC for 10 minutes and allowed to return to room temperature. No reducing agent was added. Samples of 20 µL per well were then added to a NuPAGE 4-12% Bis-Tris gel and run at 100 V for 75 minutes at room temperature. The gel was then stained with SimplyBlue Coomassie stain (ThermoFisher), de-stained overnight, and imaged on a Bio-Rad ChemiDoc MP imaging system.

2.4 Results

2.4.1 Expression and Characterization of anti-Frizzled and anti-LRP6 Fabs

DNA sequences coding for the variable regions of anti-Fzd and anti-LRP6 antibodies targeting the same receptor epitopes as the Wnt-3a ligand were taken from Gurney et al. and Jenkins et al. respectively.[40] These sequences were synthesized by Gene Universal and cloned into TGEX-FH and TGEX-LC vectors from Antibody Design Labs as described previously. We co-transfected the plasmids encoding the heavy and light chain of each Fab into suspended HEK293F cells as described in previously and purified samples as described previously. We then characterized the Fab samples by SDS-PAGE (Fig. 4a) to confirm successful expression and purification and ELISA (Fig. 4b) to confirm that the Fabs could bind specifically to their target receptor. Next, we performed luciferase assays (Fig. 4c-d) wherein either Fab was used to inhibit signaling induced by commercial Wnt. These experiments showed that the Fabs could bind to receptors on living cells and were capable of competitively inhibiting natural Wnt ligands.

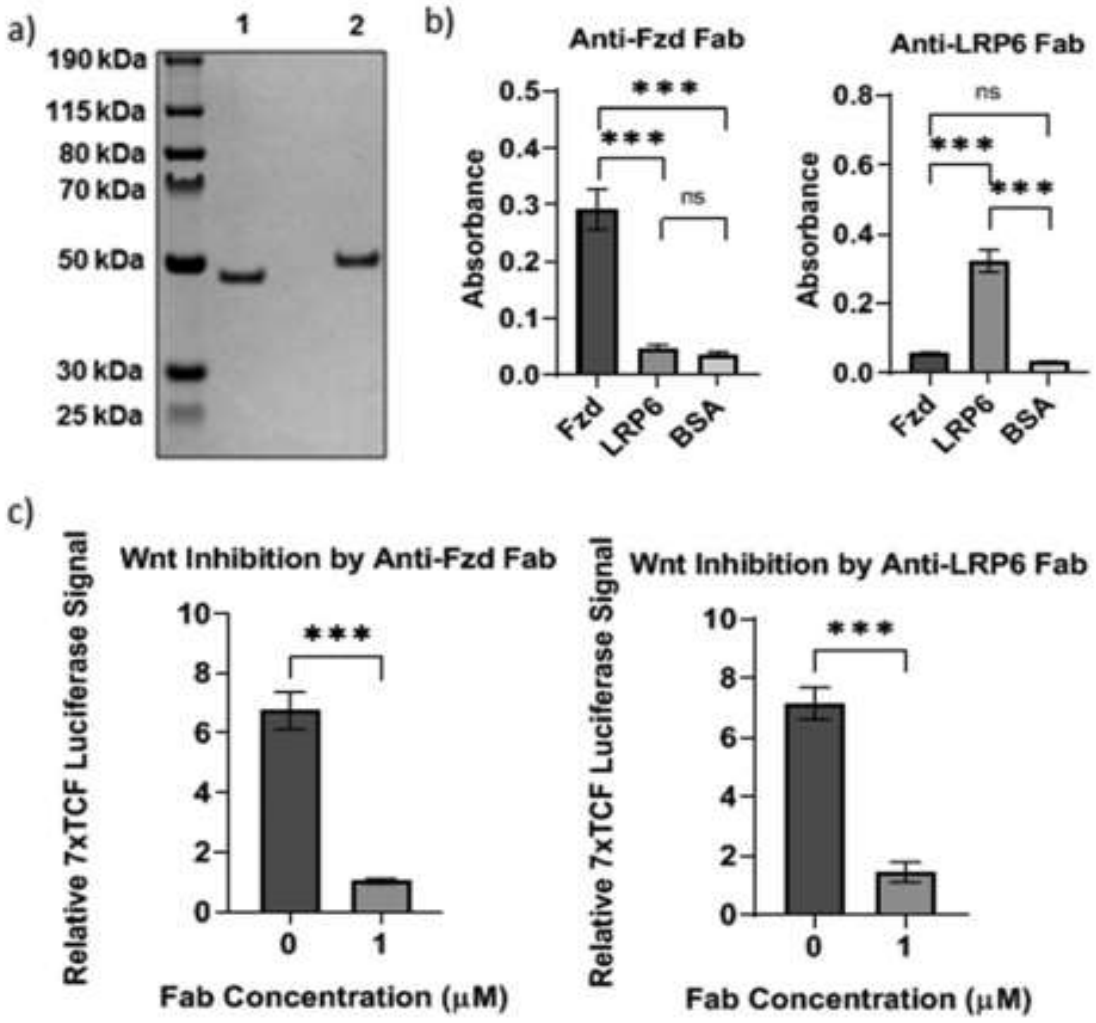

Figure 4 Characterization of expression and binding of anti-Fzd and anti-LRP6 Fabs. (a) Characterization of purified recombinant anti-Fzd Fab (Lane 1) and antiLRP6 Fab (Lane 2) by SDS-PAGE. (b) ELISAs showing specific binding of anti-Fzd and anti-LRP6 Fabs to the recombinant proteins Fzd2 and LRP6 fused to the human Fc region (Fzd2-Fc and LRP6-Fc respectively). BSA served as the negative control. ***$p < 0.0001$ by ANOVA and Tukey post hoc test; ns: not significant. (c) Luciferase assays showing level of canonical Wnt signaling activation in HEK293T cells when treated with 15 nM of exogenous Wnt-3a in the absence or presence of 1 mM anti-Fzd and anti-LRP6 Fabs respectively. ***$p < 0.0001$ by Student's t-test. Plots show mean 1 standard deviation (s.d.) Reproduced from Mukherjee et al.[28] with permission from the Royal Society of Chemistry

2.4.2 Synthesis and Characterization of Fab Heterodimer and Constituent Proteins

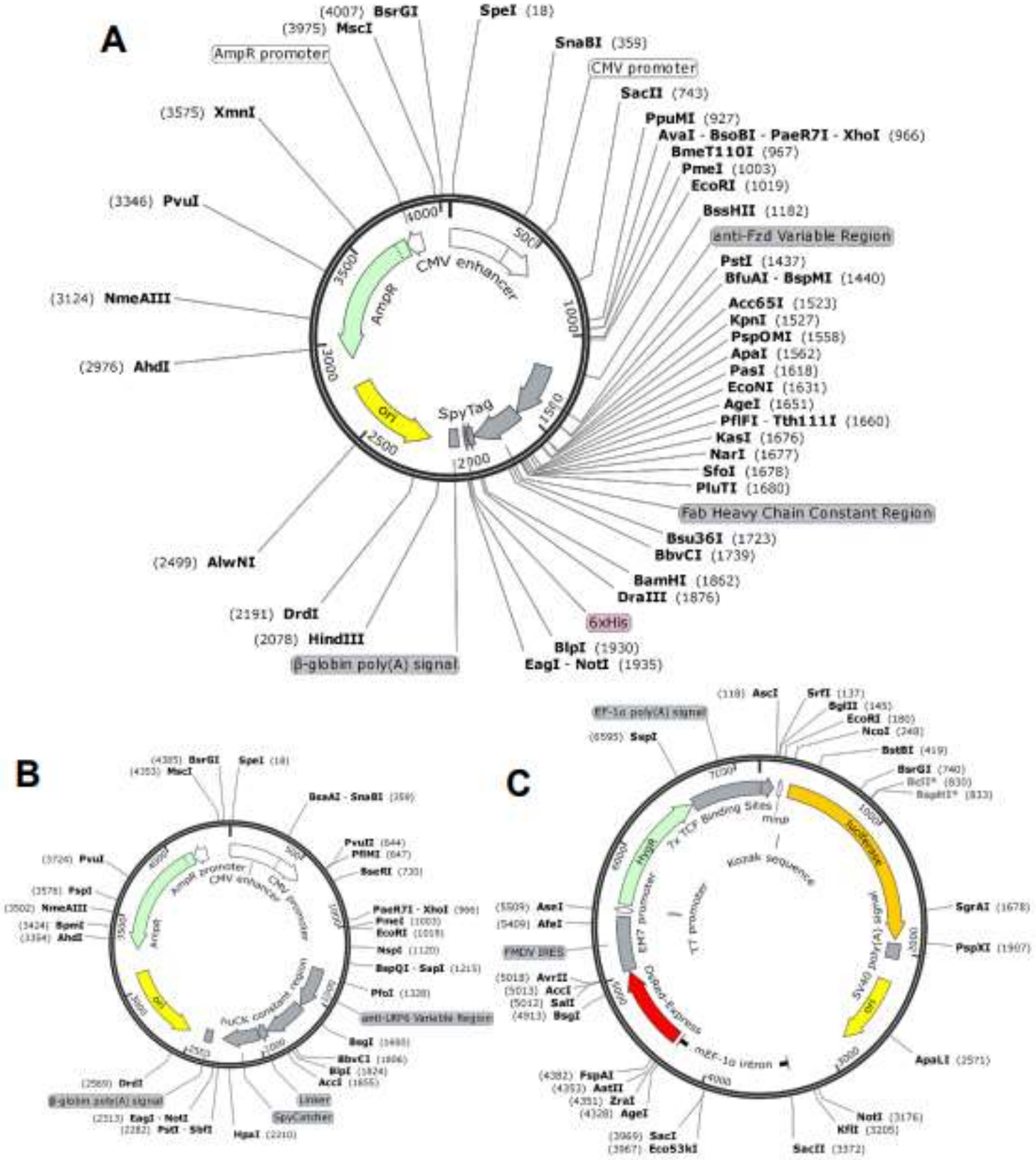

Figure 5 Vector maps for the plasmids used. A) Fzd-Fab-SpyTag in TGEX-FH; B) LRP6- Fab-SpyCatcher in TGEX-LC. C) 7x TCF Luciferase in pVitro2-hygro-DsRed. Reproduced from Mukherjee et al.[28] with permission from the Royal Society of Chemistry

To allow the linkage of the anti-Fzd and anti-LRP6 Fabs, we constructed plasmids to permit expression of a Fzd Fab with a linker and SpyTag at the C-terminus of the Fzd Fab heavy chain and an LRP6 Fab with a linker and SpyCatcher at the C-terminus of the LRP6 Fab light chain (Fig. 5). Upon mixing, the SpyCatcher and SpyTag Fab fusions form an isopeptide bond via the illustrated reaction (Fig. 6a). We expressed modified Fabs, purified them, and characterized them by ELISA (Fig. 6b). The ELISA results show that fusion of SpyTag or SpyCatcher to the Fabs do not impede their ability to bind specifically to their target receptor. Next, we mixed crude samples of the Fzd-Fab-SpyTag and LRP6-Fab-SpyCatcher proteins and incubated them for 3 hours at 37 °C to allow the SpyTag-SpyCatcher linkage reaction to proceed (Fig. 6c). We found this method improved final yield and reduced processing time compared to purifying each modified Fab separately, reacting them, and purifying again to remove unreacted monomer Fabs. To confirm successful reaction and purification, we characterized the samples by SDS-PAGE (Fig. 6d). We then further characterized the sample by dynamic light scattering (Fig. 7), Mass spectroscopy (Fig. 3), and size exclusion chromatography (SEC) (Fig. 8). We also performed an ELISA (Fig. 6e) to confirm that the heterodimer as capable of binding to both Fzd and LRP6 but not the control protein BSA.

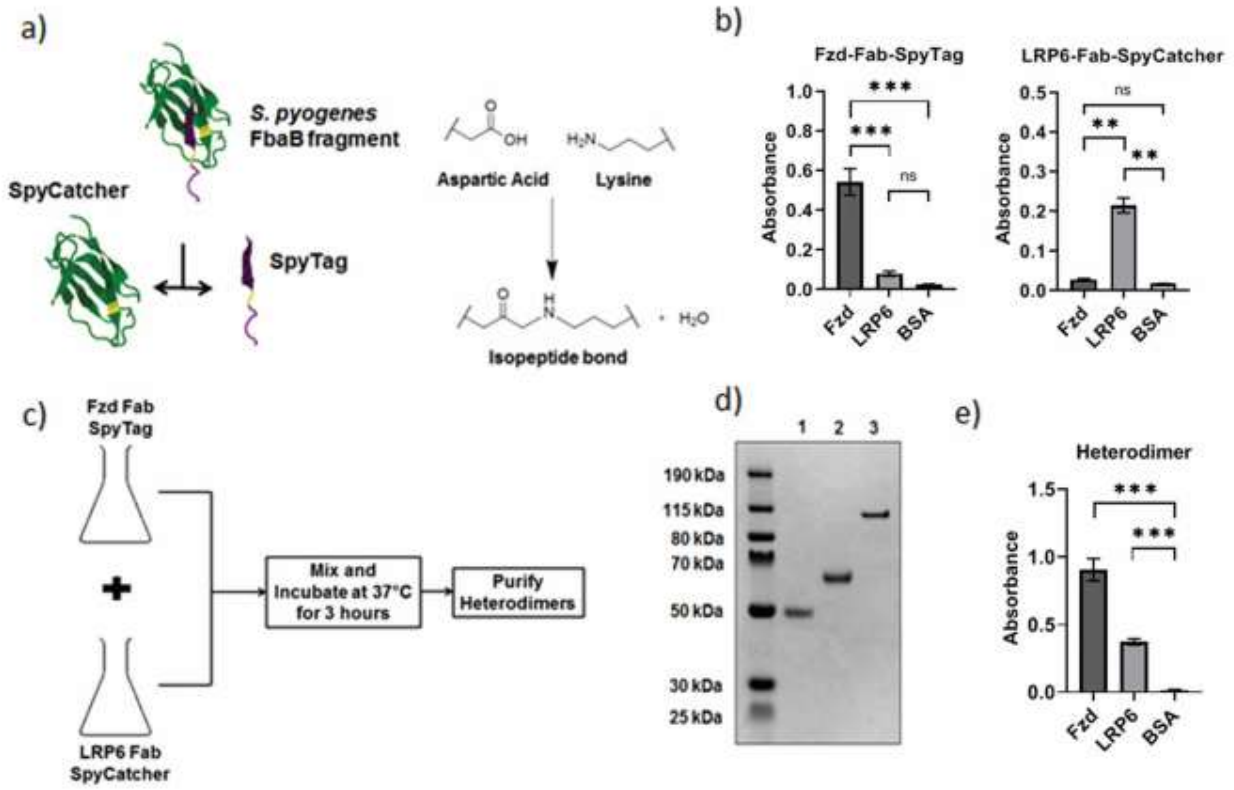

Figure 6 Synthesis and characterization of the purified Fab Heterodimer and its components. (a) Schematic showing SpyTag and SpyCatcher partner proteins isolated from S. pyogenes FbaB protein22 and reacting covalently via the formation of an isopeptide bond between them. (b) Characterization of the binding of Fzd-Fab–SpyTag and LRP6-Fab–SpyCatcher fusion proteins to Fzd2-Fc, LRP6-Fc, and BSA by ELISA. ***$p < 0.0001$, **$p < 0.01$ by ANOVA and Tukey post hoc test; ns: not significant. (c) Schematic showing the one-pot synthesis of Fzd–LRP6-Fab heterodimer from individual fusion protein components. (d) SDS-PAGE gel confirming expression and purification of Fzd-Fab–SpyTag (Lane 1), LRP6-Fab–SpyCatcher (Lane 2) and the Fab heterodimer product (Lane 3) formed from the one-pot reaction. (e) Characterization of the binding of the Fab heterodimer to Fzd2-Fc, LRP6-Fc, and BSA by ELISA. ***$p < 0.0001$ by ANOVA and Tukey post hoc test. Plots show mean 1 s.d. Reproduced from Mukherjee et al.[28] with permission from the Royal Society of Chemistry

2.4.3 Characterizing Fab Hetero-Induced Canonical Wnt Signaling Activation

To determine whether the Fab heterodimer was capable of activating Wnt signaling in living cells, we conducted a luciferase assay in which heterodimer or commercial Wnt-3a were added to HEK293T cells transfected with the 7x TCF Wnt

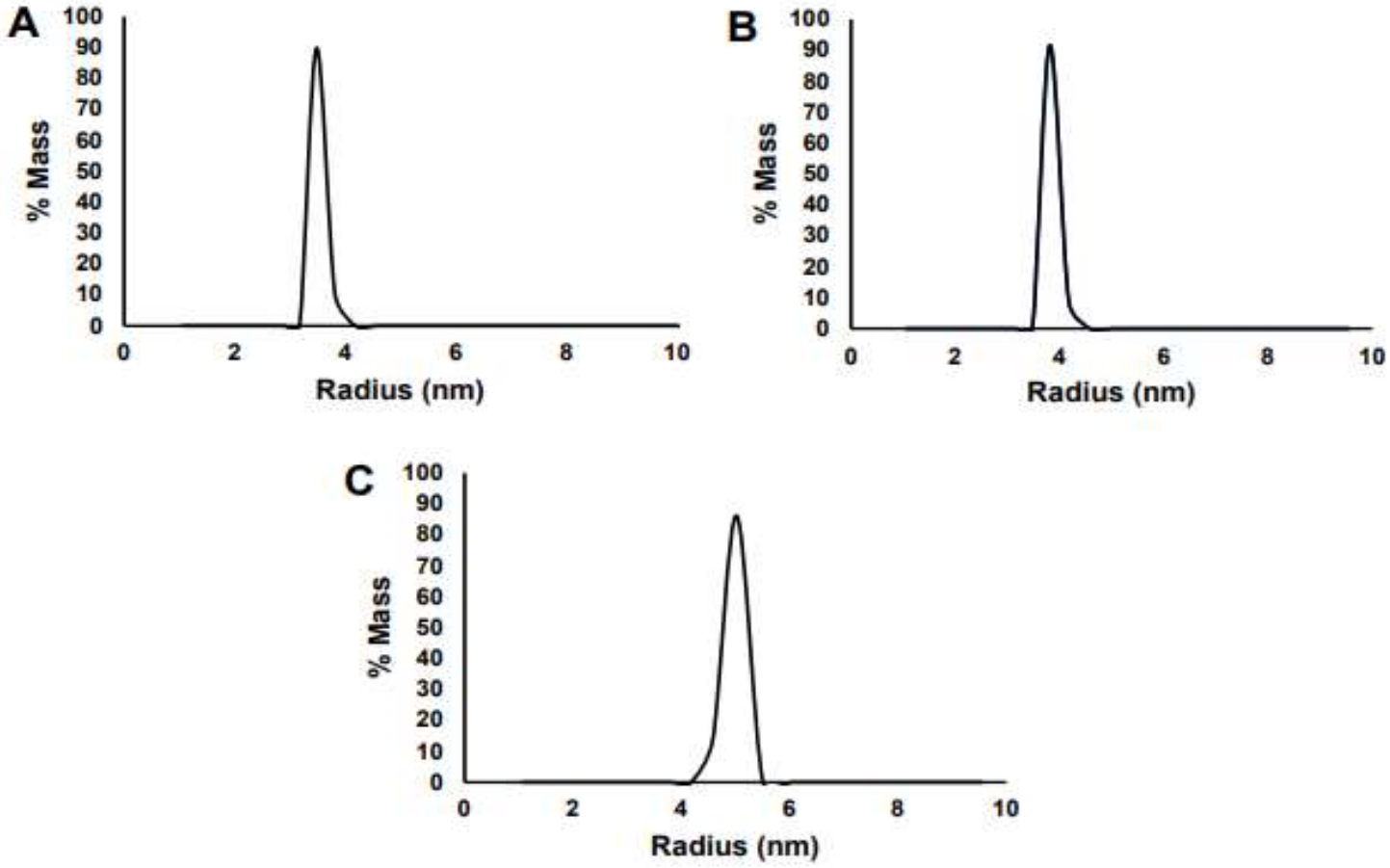

Figure 7 Characterization of Hydrodynamic Radius of Heterodimer and Monomeric Fabs. Dynamic Light Scattering analysis for purified: A) Fzd-Fab-SpyTag; B) LRP6-FabSpyCatcher; and C) Heterodimer. The data was generated from ten independent acquisitions using an isotropic sphere model. Reproduced from Mukherjee et al.[28] with permission from the Royal Society of Chemistry

reporter plasmid (Fig. 5). The synthetic heterodimer showed clear activation of canonical Wnt signaling at levels higher than those seen upon stimulation with exogenous Wnt-3a (Fig. 9a). In contrast, cells treated with Fzd-Fab-SpyTag, LRP6-Fab-SpyCatcher, or a dimer of two completely unrelated Fabs showed no significant activation of Wnt signaling. To further characterize the heterodimer, we compared the extent of Wnt signaling activation caused by Wnt-3a and the synthetic heterodimer at concentrations ranging from 0 to 15 nM (Fig. 9b). At all concentrations tested, the heterodimer induced greater fold changes in Wnt responsive luciferase signals than Wnt-3a indicating improved potency. The difference in fold change of signaling activity was greater at

lower concentrations. To further confirm that the heterodimer activates canonical Wnt signaling at the protein level, we used Western blotting to assess the levels of cytosolic β-catenin, which increase upon Wnt signaling activation by Western blot (Fig. 9c). Lysates of cells treated with 15 nM of heterodimer for 18 hours showed significantly increased levels of β-catenin compared to lysates of untreated cells confirming Wnt signaling activation. Additionally, we characterized the ability of the anti-Fzd and anti-LRP6 Fabs to inhibit Wnt signaling induced by the heterodimer. We transfected HEK293T cells with the 7x TCF Wnt luciferase reporter and treated with 15 nM of heterodimer in the absence or presence of 1 μM of either anti-Fzd Fab or anti-LRP6 Fab (Fig. 9d). The extent of signaling was significantly reduced by both Fabs compared to cells treated with heterodimer alone confirming that they competed with the heterodimer for binding to cellular Wnt receptors. This shows that covalently linking the two Fabs changes their properties by converting them from Wnt antagonists to a Wnt agonist that binds to Wnt receptors with increased avidity.

2.5 Discussion

We have developed water-soluble synthetic Fab heterodimers capable of simultaneously binding to Fzd and LRP6 to activate canonical Wnt signaling. The one-pot reaction protocol described minimizes loss due to degradation and sample processing and reduces the time and expense associated with sample purification. Furthermore, the extent of signaling induced in cells treated with the heterodimer was significantly greater than that of cells treated with commercial Wnt-3a ligand and the difference was even greater at lower doses. This approach could also be extended to other applications requiring receptor heterodimerization such as inducing signaling through G-protein

coupled receptors, activating non-canonical Wnt pathways or stimulating T cells and would allow tuning of ligand avidity. Thus, this approach could have far-reaching implications for a variety of future applications.

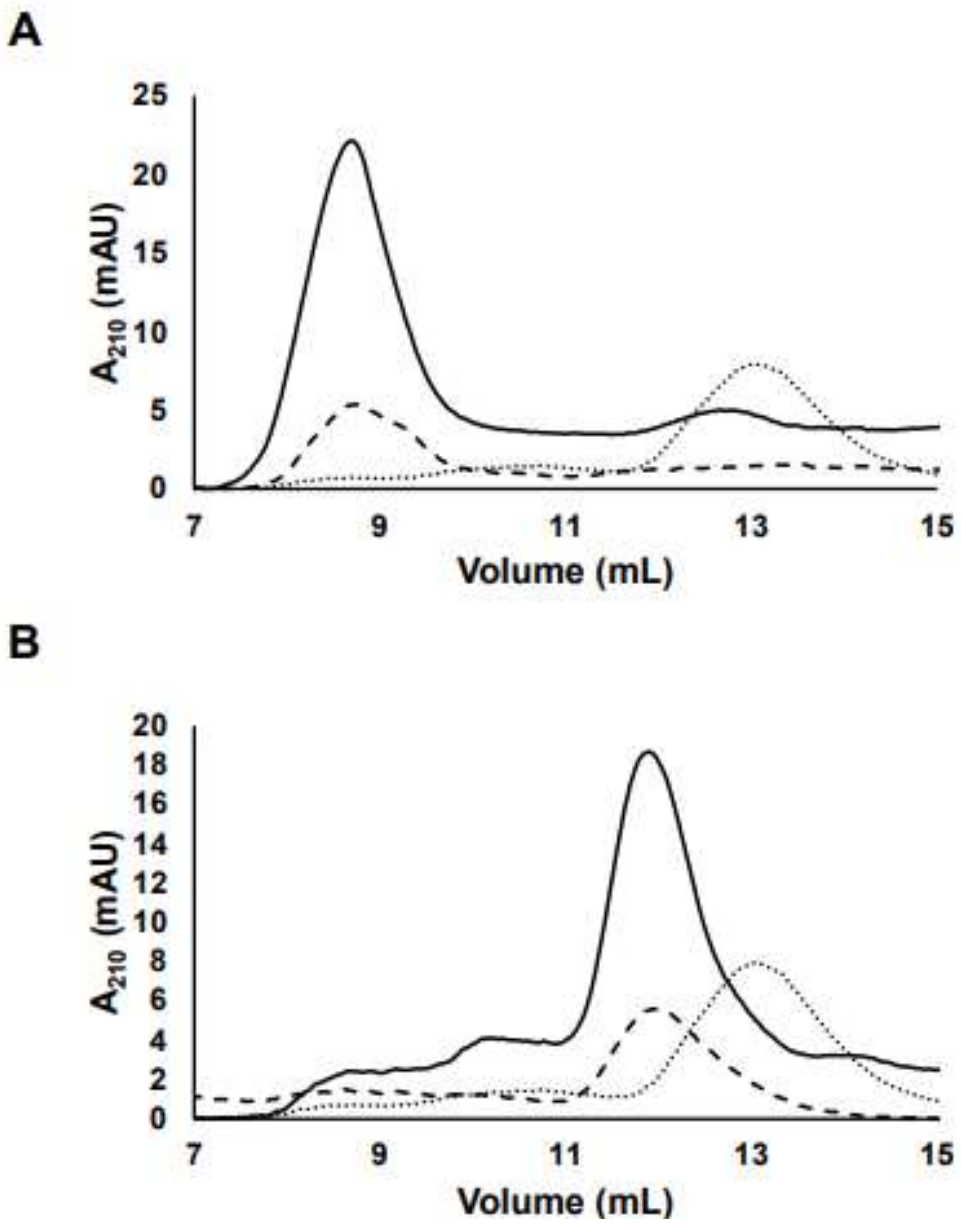

Figure 8 Characterization of Active Fraction of Heterodimer. A) Characterization by size exclusion chromatography of heterodimer alone (dotted line), LRP6-Fc (dashed line), and a mixture of heterodimer and LRP6-Fc (solid line). Analysis of peak areas suggests that 90% of the heterodimer shifts upon incubation with LRP6-Fc. B) Characterization by size exclusion chromatography of heterodimer alone (dotted line), Fzd-Fc (dashed line), and mixture of heterodimer and Fzd-Fc (solid line). Reproduced from Mukherjee et al.[28] with permission from the Royal Society of Chemistry

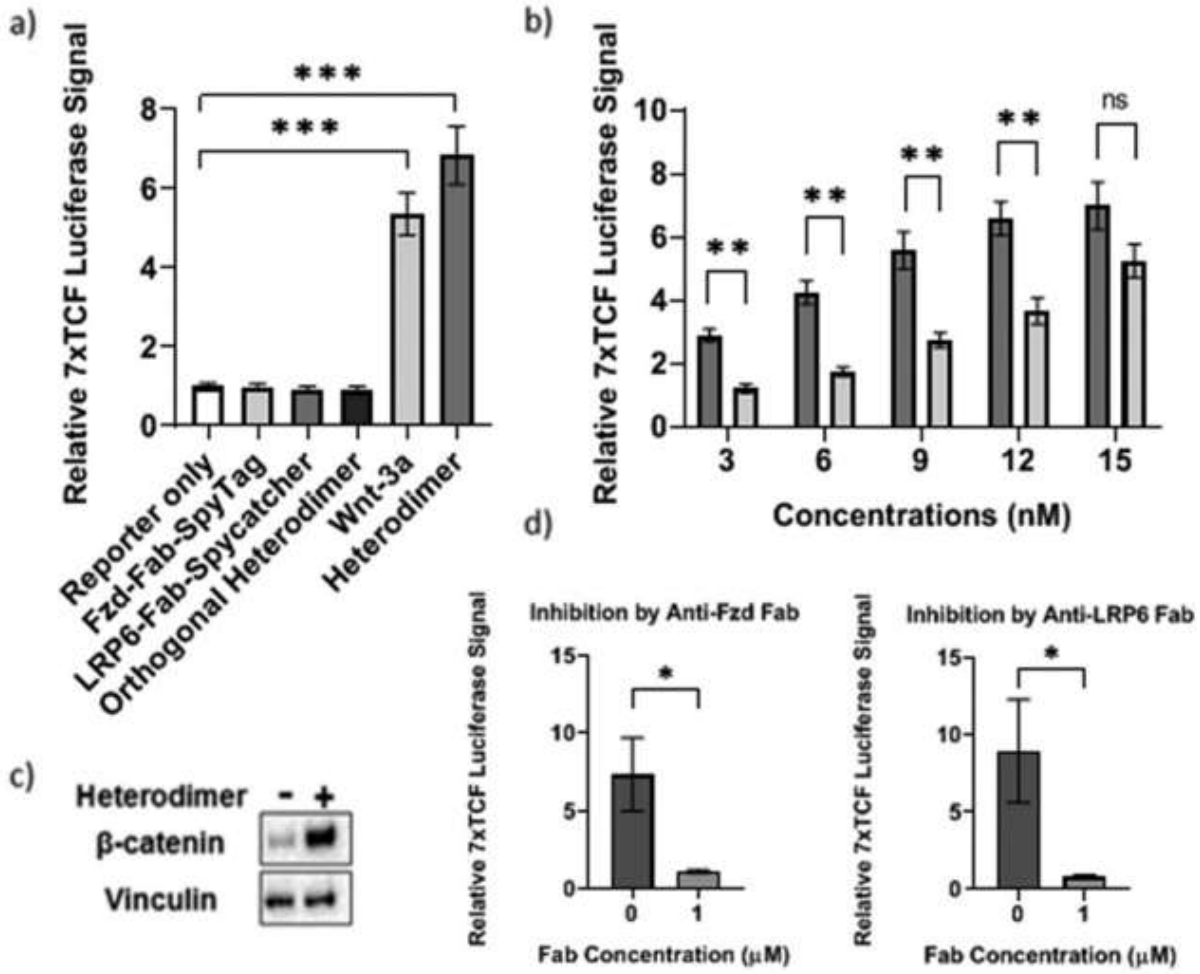

Figure 9 Characterizing Fab Heterodimer-Induced canonical Wnt signaling activation. (a) Luciferase assays showing level of canonical Wnt signaling activation in HEK293T cells when treated with 15 nM of Fab heterodimer, the component Fab fusions, Wnt-3a, and an orthogonal Fab heterodimer. ***$p < 0.0001$ by ANOVA. (b) Bar graph comparing Wnt-responsive luminescence signals at concentrations of Fab heterodimer (dark bar) and Wnt-3a (light bar) ranging from 0 to 15 nM. **$p < 0.01$ by multiple Bonferroni corrected student's t-tests; ns: not significant. (c) Western blot showing levels of cytosolic (active) b-catenin in HEK293T cell lysates in the absence () and presence (+) of 15 nM Fab heterodimer overnight. (d) Luciferase assays showing level of canonical Wnt signaling activation in HEK293T cells when treated with 15 nM of Fab heterodimer in the absence or presence of 1 mM Anti-Fzd and Anti-LRP6 Fabs respectively. *$p < 0.05$ by Student's t-test. Plots show mean 1 s.d. Reproduced from Mukherjee et al.[28] with permission from the Royal Society of Chemistry

CHAPTER 3. CONSTRUCTING A MODEL TO CLARIFY THE MECHANISM OF THE WNT SIGNALING PATHWAY[3,4]

3.1 Introduction

It is well-established that Wnt signaling causes a reduction in the degradation of β-catenin by inhibiting the activity of the destruction complex. This in turn leads to the accumulation of intracellular and nuclear β-catenin resulting in increased transcription of Wnt-regulated genes. However, there is controversy regarding the mechanism of reduction in activity of the destruction complex. Specifically, it is unknown which combination of the enzymes CK1, GSK3, and β-TrCP are impacted during Wnt signaling. It is also uncertain whether β-catenin is degraded in a processive manner in which it remains bound to the destruction complex as the enzymes modify it or in a distributive manner in which β-catenin can dissociate from the complex between each enzyme-mediated modification.

Recent research has mainly focused on two proposed mechanisms of destruction complex inactivation: inhibition of phosphorylation and inhibition of ubiquitination.[45] Li et al. performed immunoprecipitations of Axin1 and western blotting on lysates of HEK293T cells at several time points after treatment with Wnt-3a. Detection of Axin-associated destruction complex components APC and LRP6 in these experiments suggested that the destruction complex remains intact after Wnt-3a treatment. In the same

[3] I constructed the MATLAB model and performed the simulations described in this chapter. I thank my colleague Abhirup Mukherjee for generating the experimental data utilized in the model.
[4] This chapter is based on our work published in iScience:
44. Mukherjee, A.; Dhar, N.; Stathos, M.; Schaffer, D. V.; Kane, R. S., Understanding How Wnt Influences Destruction Complex Activity and β-Catenin Dynamics. *iScience* **2018,** *6*, 13-21.

immunoprecipitation experiments, Li et al. also observed increases in levels of Axin-bound CK1-phosphorylated β-catenin (CK1-p-β-catenin) and GSK3-phosphorylated β-catenin (GSK3-p-β-catenin) after Wnt-3a stimulation. However, when cells were treated with the proteasome inhibitor MG132 along with Wnt-3a and Axin1 immunoprecipitations and western blots performed, concentrations of ubiquitinylated β-catenin were reduced compared to those of cells treated with MG132 alone. Therefore, Li et al. argued that the destruction complex was inactivated by temporary saturation by GSK3-β-catenin and its activity effectively limited by the rate of β-catenin ubiquitinylation by β-TrCP.[45d] Similarly, Azzolin et al. argued that Wnt stimulation causes yes-associated protein/transcriptional coactivator with PDZ-binding motif (YAP/TAZ) to dissociate from the destruction complex which prevents β-TrCP from docking and ubiquitinylating β-catenin.[45a] In contrast, based on observations that total cytosolic β-catenin levels increased but GSK3-p-β-catenin levels decreased and then recovered after Wnt stimulation Hernandez et al. reasoned that both CK1 and GSK3 but not β-TrCP were inhibited by Wnt signaling.[45b]

To address these controversies, we (Mukherjee et al.) performed a combined experimental and theoretical analysis of Wnt pathway components which consisted of immunoprecipitation and immunoblot experiments and construction of an ordinary differential equation (ODE) kinetic model of β-catenin modification and destruction.[33] First, we treated HEK293T cells with Wnt-3a and used immunoblotting to quantify levels of total cytosolic β-catenin at several time points between zero and four hours (Figure 10A). We used concanavalin-A to remove membrane-associated β-catenin which makes up over 90% of cellular β-catenin and plays no role in Wnt signaling. In agreement with

the work of Hernandez et al.,[45b] we observed that the concentration of total cytosolic β-catenin had increased 15 minutes after Wnt-3a stimulation and reached an elevated steady

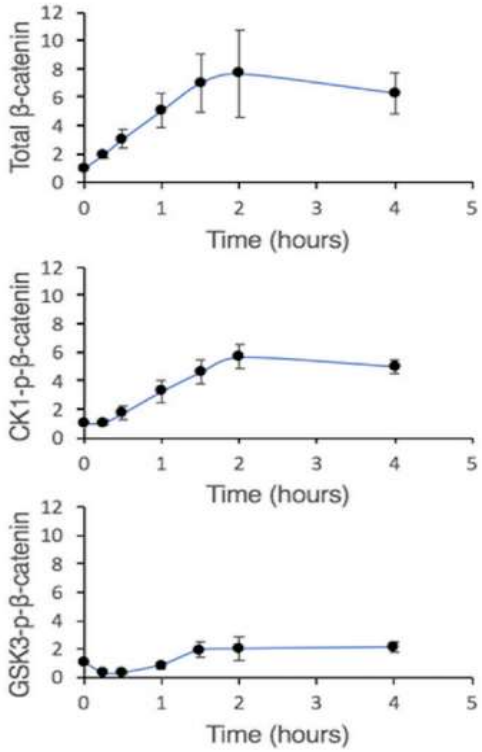

Figure 10. Characterizing β-Catenin Dynamics in Response to Wnt-3A Stimulation (A–C) Characterization of changes in the concentration of (A) non-membrane-associated β-catenin, (B) whole-cell CK1- phosphorylated-β-catenin, and (C) GSK3-phosphorylated-β-catenin with time upon Wnt stimulation through immunoblotting. Plots show mean ±1 SD (n = 3 replicates). Figure reprinted from Mukherjee et al.[14]

state concentration after approximately two hours. Since the rate of synthesis of β-catenin is unaffected by Wnt signaling, this accumulation of β-catenin suggests an initial decrease in the rate of degradation. However, the rate of β-catenin degradation must then recover to its original level two hours after Wnt stimulation to offset the rate of synthesis and produce a new steady state at an elevated β-catenin concentration. We also assessed levels of CK1-p-β-catenin upon Wnt stimulation (Figure 10B). Concentrations of CK1-p-β-catenin increased with time and also reached an elevated steady state value

approximately two hours after Wnt stimulation.[33] It should be noted that the antibody used to detect CK1-p-β-catenin targets phosphorylated serine 45 which is also present in GSK3-p-β-catenin, thus the curves described as CK1-p-β-catenin are actually CK1-p-β-catenin and GSK3-p-β-catenin combined. Nonetheless, a steady state analysis of the system shows that most of the β-catenin detected with this antibody is in fact CK1-p-β-catenin.

Next, we measured the changes in the levels of GSK3-p-β-catenin after Wnt stimulation (Figure 10C). We found the level decreased initially and then recovered to an elevated steady state after two hours. This is consistent with the inhibition of phosphorylation being responsible for the inhibition of β-catenin degradation, but is inconsistent with inhibition solely occurring downstream of phosphorylation at the ubiquitination step. As Hernandez et al noted, if inhibition occurred solely downstream of phosphorylation, then GSK3-p-β-catenin would accumulate monotonically to restore the degradation flux at a higher steady state level of this species.[45b]

To probe the mechanism responsible for inhibition of destruction complex activity we immunoprecipitated APC and measured the change in concentration of Axin1 being pulled down along with APC (Fig. 11). We chose to immunoprecipitate APC in light of reports that APC levels are significantly lower than Axin1 levels in HEK293T cells. We found there was a significant decrease in Axin1-APC interactions upon Wnt stimulation, consistent with a partial disassembly of destruction complexes.

Taken together, these experimental results suggest that upon Wnt signaling, APC and Axin1 dissociate in a fraction of destruction complexes, which inhibits their activity and leads to the inhibition of β-catenin phosphorylation and ubiquitinylation. The fraction of destruction complexes in the cytosol, however, remains structurally intact and active. The decrease in the number of active destruction complexes results in an initial decrease in the rate of β-catenin degradation and thus an increase in the intracellular concentration of β-catenin. Mass action then causes an increase in the rate of β-catenin phosphorylation by the remaining active destruction complexes. At the new steady state following Wnt stimulation, the rate of degradation of β-catenin would once again equal the rate of synthesis and the flux through the destruction complexes would return to its original value.

Figure 12A depicts the sequence of intracellular β-catenin modifications. We applied a Michaelis-Menten model to the activity of CK1 while assuming that the

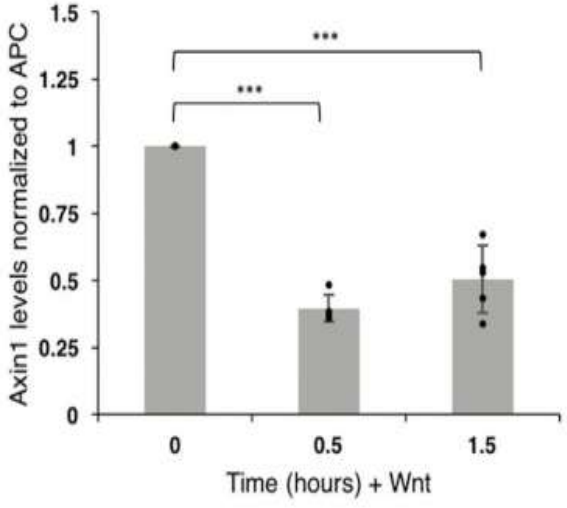

Figure 11. Characterization of Destruction Complex Components upon Wnt Stimulation Quantifying changes in Axin1-APC interactions upon Wnt stimulation. Plot shows mean ±1 SD (n = 5 replicates), ***p < 0.001 by a two-tailed t test. Figure reprinted from Mukherjee et al.[14]

cytosolic β-catenin concentration was low compared to the Michaelis constant (K_{M1}).[45b] CK1 activity was therefore given by $(k_{cat1}/K_{M1})[DC][B_0]$ where k_{cat1} is the catalytic rate of CK1α on the destruction complex, [DC] is the concentration of the destruction complexes, and [B0] is the concentration of unphosphorylated β-catenin. In Figure 12A, the rate constant k_1 is given by $(k_{cat1}/K_{M1})[DC]$. In our model, when Wnt stimulation inhibits the activity of the destruction complex [DC] effectively decreases and therefore $[B_0]$ must increase to allow the rate of CK1 phosphorylation $(k_{cat1}/K_{M1})[DC][B_0]$ to recover to its original value (Fig. 12B).

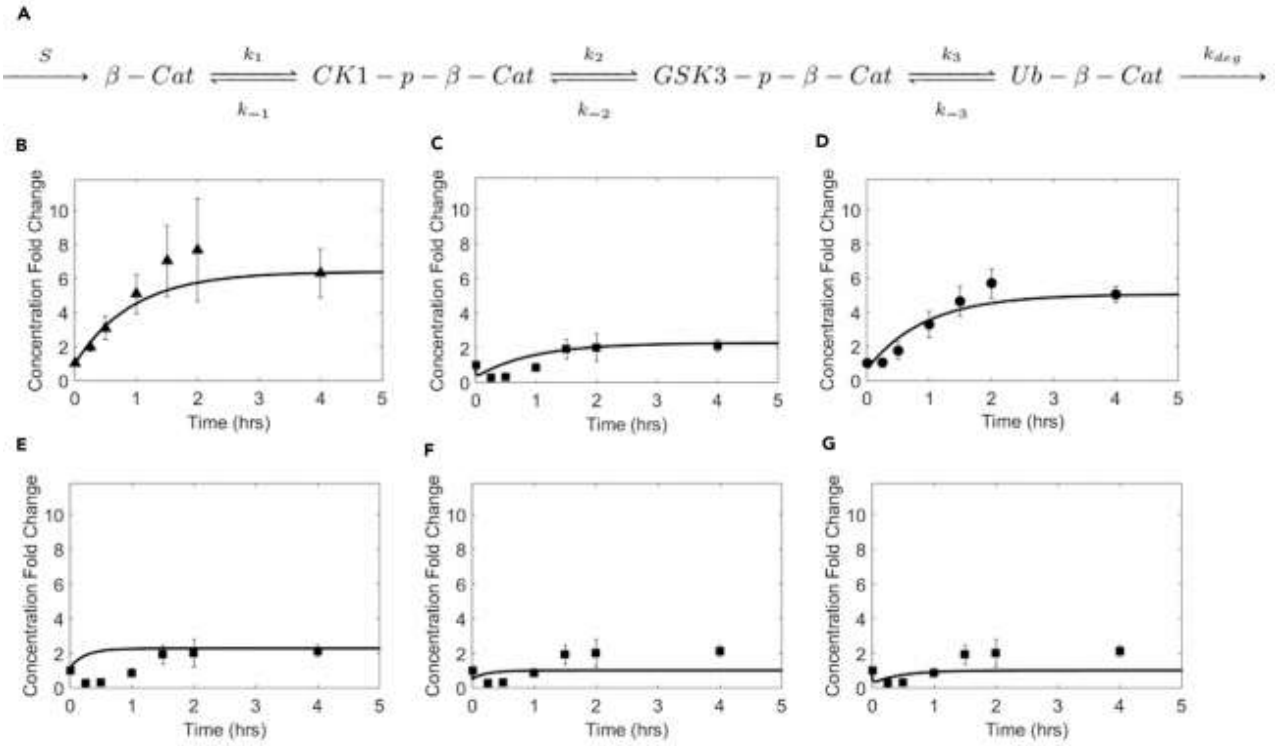

Figure 12. Modeling β-catenin Dynamics in Response to Wnt Stimulation A) Cartoon showing sequential enzymatic modifications of β-catenin. (B–D) Comparison of results from numerical integration of rate equations with experimental data for changes in concentrations of B) total β-catenin, C) GSK3-p-β-catenin, and D) CK1-p-β-catenin. Values of the rate constants (k_1, k_2, and k_3) were each assumed to decrease to 0.44 times their original value, to reflect the decrease in the number of active destruction complexes. (E–G) Comparison of results from numerical integration of rate equations with experimental data for changes in concentrations of GSK3-p-β-catenin for a decrease in the value of E) only k_3, F) only k_2, and G) k_1 and k_2, but not k_3. Experimental data in plots (B–G) show mean G1 SD (n = 3 replicates). Figure reprinted from Mukherjee et al.[14]

We next used our results to analyze whether the destruction complex activity was processive or distributive. The generally accepted view is that the destruction complex is processive, with β-catenin undergoing a series of phosphorylations before being released from the complex. However, our results — which suggest inhibition of phosphorylation due to partial disassembly that causes a decrease in the number of active destruction complexes — are inconsistent with this view. As explained by Hernandez et al., in the processive case, CK1-p-β-catenin would remain bound to the destruction complex before its phosphorylation by GSK3.[45b] Therefore, the rate of GSK3 phosphorylation would be (k_2)[CK1-p-β-catenin]. The rate constant for GSK3 phosphorylation, k_2 (Figure 12A), would then be independent of [DC] ($k_2 = k_{cat2}$). The concentration of CK1-p-β-catenin at the new steady state should therefore return to its original value, so that the rate of GSK3 phosphorylation (k_2[CK1-p-β-catenin]) also recovers. However, we see a significant (approximately 5-fold) increase in the concentration of CK1-p-β-catenin upon Wnt stimulation (Figure 12B), similar to the significant increase in concentration of total β-catenin. This increase is inconsistent with a processive model and instead supports a distributive model for destruction complex activity, with the increase in CK1-p-β-catenin concentration being necessary to compensate for the decrease in [DC]. CK1-p-β-catenin would therefore be present in both free and destruction-complex-bound states.

As seen in Figure 12C, the concentration of GSK3-p-β-catenin at the new steady state (following Wnt stimulation) is also greater than its initial value. This suggests that GSK3-p-β-catenin is also present in both free and destruction-complex-bound states. Moreover, these results are consistent with ubiquitination occurring primarily in an intact destruction complex as suggested by Li et al. (2012).[45d] An increase in the total

concentration of GSK3-p-β-catenin would be required if ubiquitination were occurring primarily in the destruction complex, to compensate for the decrease in the number of active destruction complexes upon Wnt stimulation. In contrast, if ubiquitination were occurring primarily outside the destruction complex, we would not expect to see an increase in total levels of GSK3-p-β-catenin at the new steady state.

3.2 Modeling of β-catenin Dynamics in Response to Wnt Stimulation

To further explain these experimental results we constructed a simple ordinary differential equation (ODE) model to describe the kinetics of β-catenin phosphorylation and ubiquitinylation based on a similar model created by Hernandez et al. In this model, B_0, B_1, B_2 and B_3 represent unphosphorylated β-catenin, CK1-phosphorylated β-catenin, GSK3-phosphorylated β-catenin, and ubiquitinylated β-catenin respectively.[45b] S represents the rate of synthesis of β-catenin, $[B_i]$ denote concentrations (i = 0, 1, 2, 3), and k_{deg} and k_j (j = ±1, ±2, ±3) denote rate constants. The model could be extended to other cell types, but it would be necessary to determine the values of the rate constants and the synthesis rate of β-catenin for the new cell type.

In this model, post-translational modifications of β-catenin are reversible first order processes with forward rate constants representing the activity of CK1, GSK3 and β-TrCP and reverse rate constants representing the activity of phosphatases and de-ubiquitinases. The phosphorylation and degradation of β-catenin was modeled using the following dynamical equations:

1) $\frac{d[B_0]}{dt} = S - k_1[B_0] + k_{-1}[B_1]$

2) $\frac{d[B_1]}{dt} = k_1[B_0] - (k_2 + k_{-1})[B_1] + k_{-2}\,[B_2]$

3) $\frac{d[B_2]}{dt} = k_2[B_1] - (k_3 + k_{-2})[B_2] + k_{-3}\,[B_3]$

4) $\frac{d[B_3]}{dt} = k_3[B_2] - (k_{deg} + k_{-3})[B_3]$

We used our results to predict β-catenin dynamics in response to Wnt signaling (Figures 12B–12D). In our proposed distributive model, the response to a Wnt signal is caused primarily by a decrease in the number of active destruction complexes, which causes a decrease in magnitudes of the rate constants for phosphorylation and ubiquitination – k_1, k_2, and k_3 (Figure 12A). Original values of these rate constants were taken from Hernandez et al.[45b] The lines in Figures 12B–12D represent β-catenin concentrations obtained by numerical integration of the dynamical equations (see equations 1–4) with the value of each of the rate constants k_1, k_2, and k_3 after Wnt stimulation being changed to 0.44 times their value before Wnt stimulation. The choice of 0.44 was guided by our experimental data (Figure 11). The average Axin1/APC ratio upon Wnt stimulation determined from APC-Axin1 co-immunoprecipitation experiments, ranged from ca. 0.39 to 0.5 times its value before Wnt stimulation and 0.44 lies in this range and is close to the average of these two values. As seen in Figures 12B–12D, the predicted changes in steady-state concentrations and the dynamical behaviors match the experimental results. In contrast, predictions based on inhibition of only ubiquitination (Figure 12E) or only phosphorylation (Figures 12F and 12G) do not explain the experimental results for GSK-3-p-β-catenin dynamics. If only ubiquitination is inhibited, results obtained by numerical integration of the dynamical equations do not show a dip in

the concentration of GSK3-p-β-catenin (Figure 12E). If only phosphorylation is inhibited, but not ubiquitination (Figures 12F and 12G), then GSK3-p-β-catenin levels at the new steady state would recover to their initial value, but not exceed it, in contrast to experimental results. We note that whereas our experimental data are most consistent with a mechanism based on the inhibition of both phosphorylation and ubiquitination (Figure 12), our simulations do not perfectly match the experimental time course for recovery of GSK3-p-β-catenin concentrations. This difference could be due to factors not accounted for in our simple model. For instance, the inhibition could occur with a slight lag, and at different rates in different cells, due to heterogeneity in the time taken for Wnt to diffuse and bind to receptors on different cells and in the time required for complex disassembly.

3.3 Conclusion

In summation, our results support the following mechanistic model for Wnt signaling. After Wnt stimulation, approximately 44% of the destruction complexes relocate to the membrane, and this relocation subsequently leads to the disassembly of these destruction complexes. The remaining destruction complexes remain intact and active in the cytoplasm. However, the initial decrease in the number of active destruction complexes results in an initial decrease in the rate of degradation of β-catenin. Consequently, free β-catenin is able to accumulate, until mass action results in an increase in the levels of destruction-complex-bound GSK3-p-β-catenin and a recovery of the rate of degradation of β-catenin, but at an elevated steady-state level of β-catenin. Understanding this fundamental mechanism provides a rational basis for tuning the pathway for scientific and therapeutic purposes.[8, 46]

CHAPTER 4. CHARACTERIZATION OF THE EFFECTS OF RATIONALLY DESIGNED OPTOGENETIC PHOTOSWITCHES ON WNT SIGNALING[5]

4.1 Description of Engineered Photoswitches

Optogenetics employs light-sensitive proteins such as *Arabidopsis thaliana* cryptochrome 2 (Cry2) to study a variety of cellular processes. The use of light in such applications is advantageous because it is generally bio-orthogonal, it allows precise spatiotemporal control of stimulation, and it can be turned on or off quickly and easily to facilitate studies of kinetics. Optogenetics can be used to study cellular signaling by generating fusion proteins consisting of cellular receptors linked to Cry2 which can be used to induce signaling in a light-dependent manner.[47] A noteworthy example involved the construction of a fusion of the photolyase homology region (PHR) domain of Cry2 with the intracellular domain of LRP6 (termed Cry2PHR-mCherry-LRP6c) by Bugaj et al.[48] This fusion protein was shown to be capable of activating Wnt signaling in a light-dose-dependent manner. To improve the versatility of this tool we generated variants of **C**ry2PHR-mCherry-**L**RP**6**c with **N** **m**utated PPPAP motifs (CL6mN) to eliminate Wnt signaling activities. The dissociation half-lives of these variants can be tuned by varying the number of PPPAP motifs, with the half-life increasing as much as 6-fold for a variant with five motifs (CL6m5) relative to Cry2PHR. We also demonstrated the compatibility of CL6mN with previously reported Cry2-based photoswitches.[47]

[5] This chapter is based on our work published in ACS Synthetic Biology:
47. Mukherjee, A.; Sudrik, C.; Hu, Y.; Arha, M.; Stathos, M.; Baek, J.; Schaffer, D. V.; Kane, R. S., CL6mN: Rationally Designed Optogenetic Photoswitches with Tunable Dissociation Dynamics. *ACS Synthetic Biology* **2020,** *9* (9), 2274-2281.

4.2 Methods

4.2.1 Mammalian Cell Culture for Luciferase Assay to Characterize Activation of Canonical Wnt Signaling

HEK293T cells were purchased from the American Type Culture Collection (ATCC) and cultured in Dulbecco's Modified Eagle Medium (DMEM) (high-glucose) supplemented with 10% heat-inactivated fetal bovine serum (HI-FBS) (Gibco, Thermo Scientific) in a humidified incubator at 37 °C with 8% CO_2 concentration. For the luciferase assay, the cells were subcultured and plated onto a 6-well plate coated with poly-L-lysine and grown up to approximately 90% confluency. The cells were then co-transfected with the Wnt-responsive 7×TFP reporter plasmid and a plasmid of interest at a w/w ratio of 1:1 using Lipofectamine 2000 (Thermo Scientific) according to the manufacturer's protocol. The cells were trypsinized again approximately 18−24 h after transfection using 0.25% Trypsin- EDTA (Thermo Scientific), and re-plated in two 96-well plates (Greiner Bio-One) coated with poly-L-lysine (Sigma-Aldrich). One of these 96-well plates was kept in the dark while the other one was irradiated with blue light pulses from LEDs attached to an Arduino UNO board. The pulses were turned ON for 0.5 s and turned OFF for 0.5 s. After treatment, cells were analyzed using a luciferase assay to check for Wnt signaling activity.

4.2.2 Assay to Characterize Activation of Noncanonical Wnt Signaling

HEK293T cells were subcultured and plated onto a 6-well plate coated with poly-L-lysine and grown up to approximately 90% confluency. Cells were co-transfected using Lipofectamine 2000 at a w/w ratio of 1:2:3 respectively with plasmids encoding a

4× CBF1, Suppressor of Hairless, Lag-1 (CSL) luciferase reporter, a 3×FLAG Notch1 intracellular domain, and either Wnt-5a, CL6m5 , or mCherry based on protocols from Ann et al. 4×CSLluciferase was a gift from Raphael Kopan (Addgene plasmid # 41726; http://n2t.net/addgene:41726; RRID:Addgene_41726), 3×FlagNICD1 was a gift from Raphael Kopan (Addgene plasmid # 20183; http://n2t.net/addgene:20183; RRID:Addgene_20183), and pcDNA-Wnt5A was a gift from Marian Waterman (Addgene plasmid # 35911; http://n2t.net/ addgene:35911; RRID:Addgene_35911). After transfection, cells were kept in the dark. After 24 h cells were split into 96-well plates and cultured for another 24 h. The cells were then treated with 1 s pulses of blue LED light every 5 s for 24 more hours. Cells were washed three times with Dulbecco's phosphate-buffered saline (DPBS) (ThermoFisher), lysed by incubating with 30 μL of passive lysis buffer (Promega) on a rocking platform for 15 min and centrifuged at 1000×g to remove debris. The lysate was then transferred to an opaque white 96-well plate. Luminescence was read on a plate reader immediately after addition of 100 μL per well of firefly luciferase assay substrate (Promega).

4.3 Assessing the Effects of Optogenetic Photoswitches on Wnt Signaling

Since these photoswitches contained mutants of LRP6, it was conceivable that they might induce undesired cell signaling upon light-induced clustering. To assess the extent of this aberrant signaling we performed luciferase assays on HEK293T cells co-transfected with a non-canonical Wnt pathway reporter plasmid and a plasmid encoding CL6m5, mCherry, or Wnt-5a (Fig. 13). We found that the luciferase signal in the CL6m5 group was comparable to that of the mCherry control group and significantly less than

that of the for cells transfected with Wnt-5a, suggesting that CL6m5 did not activate non-canonical Wnt signaling.

Next, we wanted to ensure that these photoswitches did not interfere with the ability of cells to undergo signaling induced by canonical Wnt ligands. To test this we performed luciferase assays on HEK293T cells transfected with plasmids encoding CL6m3, CL6m5, or mCherry in the presence or absence of exogenous Wnt-3a (Fig. 14). All groups showed significant signaling activity in the presence of Wnt-3a and the extent of signaling was comparable between groups. These results suggest that CL6mN does not have an appreciable effect on ligand-induced canonical Wnt signaling.

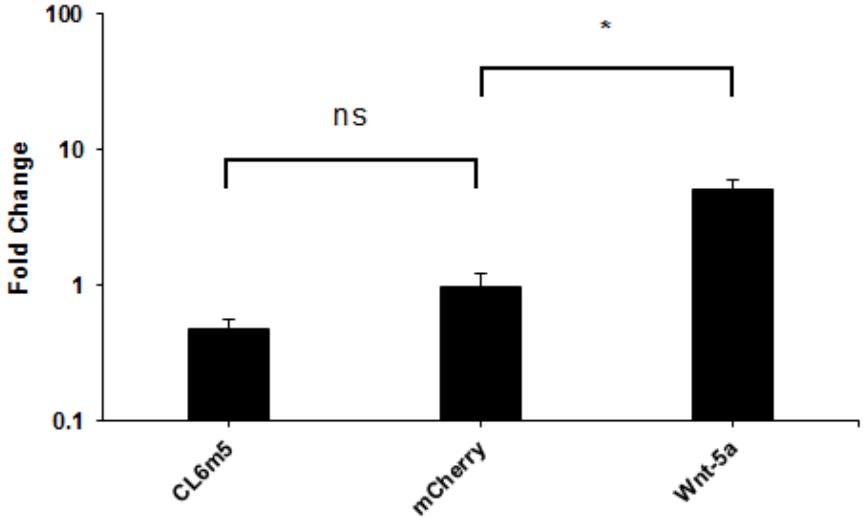

Figure 13. Characterization of the effect of CL6m5 on non-canonical Wnt pathways. A luciferase assay was used to probe the activation of non-canonical Wnt signaling. While activation was seen for cells transfected with plasmids encoding Wnt-5a, no significant activation was observed in cells transfected with plasmids encoding CL6m5 (relative to controls: cells transfected with plasmids encoding mCherry). (*: $p < 0.05$, ns: not significant n = 3 replicates, One-way ANOVA with Tukey post hoc test

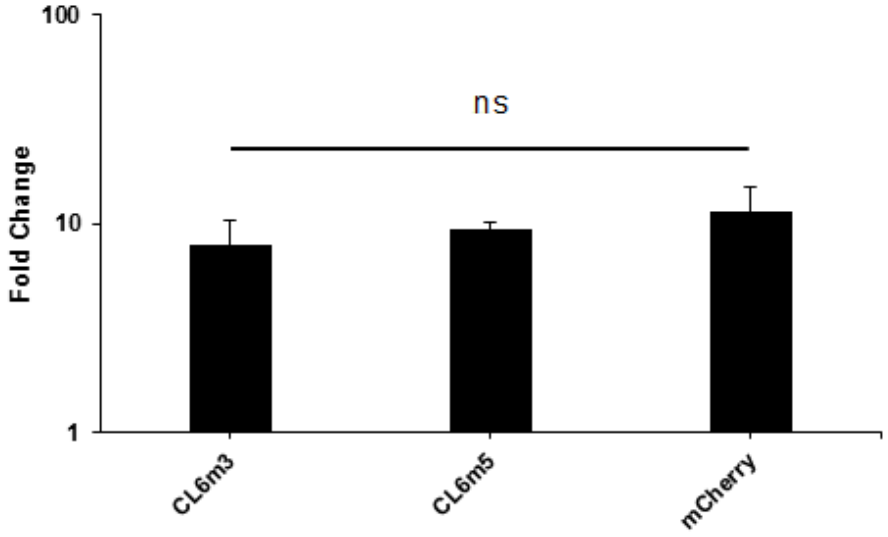

Figure 14. Characterization of the ability to activate Wnt signaling in CL6mN-transfected cells. A luciferase assay was used to probe the activation of canonical Wnt signaling. Data are normalized relative to those for cells not treated with Wnt-3a. Significant activation was observed for cells transfected with plasmids encoding CL6m3, CL6m5, or mCherry (control) when treated with 15 nM commercial Wnt-3a ligand compared to untreated cells. However, there was no significant difference in the extent of activation between groups (ns: not significant, n = 3 replicates, One-way ANOVA)

CHAPTER 5. CREATING REPORTER CELL LINES TO TRACK DIFFERENTIATION OF IPSCS INTO CARDIOMYOCYTES

5.1 Introduction

5.1.1 Motivation

Cardiovascular disease is the number one cause of death in the United States and most of these deaths are due to myocardial infarctions.[49] These are caused by the rupture of atherosclerotic plaques composed of cholesterol, lipids, and monocyte-derived macrophages in the coronary arteries. These plaques inevitably build up with age and upon reaching a critical size they are ruptured by shear stress caused by blood flow. This rupture causes a blood clot to form which blocks blood flow to the heart. The resulting ischemia typically kills approximately one billion ventricular cardiomyocytes drastically reducing the performance of the heart.[50] Unfortunately, adult cardiomyocytes have essentially no capability to proliferate and replace the lost cells. Therefore there is great interest in stem cell-based approaches to re-grow these cells efficiently at a large scale so they can be grafted onto an infarcted heart to restore function.

Hundreds of protocols have been developed to generate cardiomyocytes from stem cells. Many of these protocols involve the carefully timed addition of specific doses of protein ligands or small molecules that modulate Wnt, transforming growth factor beta (TGF-β), or retinoic acid signaling pathways.[51] Others make use of physical cues such as substrate stiffness or topology, feeder cells, electrical stimulation or regulatory RNAs.[51] The method developed by Lian et al., is particularly noteworthy for its novelty, simplicity

and high cardiomyocyte purity.[4] This method controls the differentiation of induced pluripotent stem cells (iPSCs) into cardiomyocytes by temporally modulating only the Wnt signaling pathway (Figure 15)[52]. These cells are first treated with the small molecule

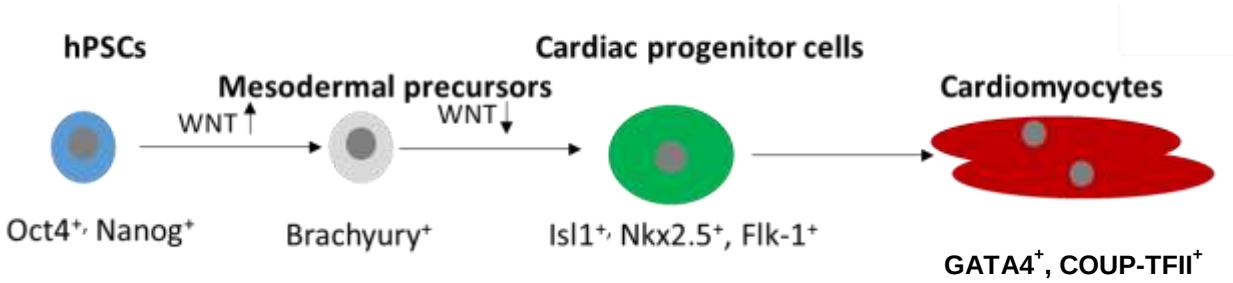

Figure 15 Differentiation of iPSCs into Cardiomyocytes. Activation of Wnt signaling in iPSCs leads to Brachyury expression and a mesodermal fate. Subsequent inhibition of Wnt signaling under the appropriate culture conditions is sufficient to direct differentiation toward cardiac progenitors and eventually cardiomyocytes.

Wnt signaling activator CHIR99021 and several days later treated with the small molecule Wnt signaling inhibitor known as inhibitor of Wnt processing and secretion 2 (IWP-2). However, the cardiomyocytes generated by this or similar approaches are of a heterogeneous fetal phenotype rather than a homogenous adult phenotype. Consequently, they do not generate sufficient force upon contraction and are prone to arrhythmia.[53]

To address this issue, we have combined reporter genes, CRISPR/Cas9 genome editing techniques, knowledge of cardiac development, and established cardiomyocyte differentiation protocols to create genome-edited reporter cell lines. These cell lines permit continuous *in situ* monitoring of co-cultured wild type cells. Readouts from reporter assays would be helpful in characterizing the activity of critical developmental marker genes in heterogeneous iPSC-derived cardiac cell populations. This information would provide feedback which would better inform optimization of differentiation

protocols and which could be used for quality assurance purposes during the manufacturing of therapeutic cells.

Since these reporter cells are ultimately meant for *in situ* monitoring of therapeutic cells and there potential safety concerns associated with gene edited cells, an inducible suicide mechanism will be employed to safely remove these edited cells from co-culture upon completion of the differentiation process. It is important that this mechanism work rapidly and robustly without harming wild type cells in the co-culture.

5.1.2 Reporter Genes and Biosensors to Study Development

In order to better understand signaling pathways such as Wnt or to quantify their extent over time, several so-called reporter genes are employed. These generally include a wide variety of fluorescent proteins, oxidative enzymes known as luciferases which react with small molecule substrates to produce light, or other enzymes such as β-galactosidase which reacts with its substrate to produce a color change.

One common use of these reporter genes is to place them downstream of a promoter of a target gene in a plasmid so that when the target gene is expressed the reporter will be as well. Similarly, by including several appropriately spaced transcription factor binding DNA sequences upstream of a minimal promoter and a reporter gene, the extent of activation of particular signaling pathways can be measured. Yet another approach is to transfect cells with a plasmid containing a DNA sequence enabling expression of a fusion protein consisting of a target protein and reporter protein directly linked by a flexible peptide sequence.

Generally enzymes are used to study signaling pathway or promoter activity. This is because one enzyme molecule can rapidly catalyze a reaction with a large number of substrate molecules to produce a strong signal. Fluorescent proteins can be used in this way as well but generally offer lower sensitivity. Fluorescent proteins are more commonly used as fusions to the target gene because this enables easy visualization. These markers can also be used for cell sorting if desired.

These reporter systems are often used in short-term transient transfection experiments. However, they can also be incorporated into the genome via lentiviral transduction, site specific recombination, or CRISPR/Cas9. This approach is more time-consuming but allows the creation of stable cell lines (or even animal models) which produce a more consistent signal without the need for repeated transfections. This approach can also be used for longer term experiments such those involving stem cell differentiation.

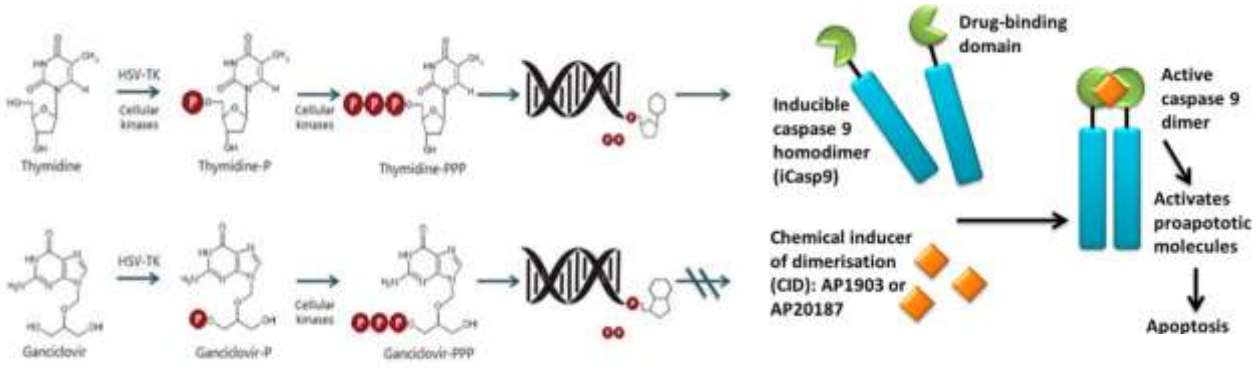

Figure 16 Mechanisms of Action of Inducible Cell Suicide Genes. A) Thymidine can be phosphorylated by HSV-TK or Cellular kinases in order to be incorporated into DNA during replication. Ganciclovir can similarly be phosphorylated by HSV-TK and incorporated into DNA terminating replication and triggering apoptosis (Figure reprinted from Rangel-Sosa et al. Colombia Medica 2017)[54] B) The engineered protein iCasp9 can be activated by a small molecule dimerizer to trigger apoptosis. (Figure reprinted from Gargett et al. Front. Pharmacol. 2014)[55]

5.1.3 Validation of an Inducible Suicide Switch to Safely and Specifically Eliminate Gene Edited Cells from Co-culture

One popular method of inducing suicide in cells is the use of pro-drugs. Pro-drugs are non-toxic small molecules that are metabolized to form a toxin in the presence of a protein encoded by a "suicide gene". A prominent example of a suicide gene is one that encodes Herpes Simplex Virus Thymidine Kinase (HSV-TK)[54] (Figure 16A). Like mammalian kinases, this protein phosphorylates thymidine which allows the nucleotide to be incorporated into DNA during replication. However, HSV-TK can also phosphorylate a similar small molecule known as ganciclovir. When phosphorylated ganciclovir is incorporated into DNA during replication it terminates the process which leads to apoptosis. Endogenous mammalian kinases are unable to phosphorylate ganciclovir which prevents it from harming wild type cells.

Another commonly employed method for generating cells which can be induced to undergo apoptosis involves the incorporation of genes encoding inducible caspases. Inducible caspases are engineered proteins that can induce apoptosis in the presence of small molecules. A well-known example is inducible caspase 9[55] (Figure 16B). When a domain of the drug binding protein FK506 is fused to caspase 9, it can be dimerized by the small molecule AP1903. This dimerization in turn activates caspase 3 which directly leads to apoptosis.

5.1.4 Cardiomyocyte Development

Mammalian embryonic development begins with the fertilization of an ovum by a spermatozoon to form a zygote. After three to four days, this zygote then divides into a

solid 16 cell sphere known as a morula. Next, the solid mass of cells becomes a hollow sphere with an inner cell mass (ICM) known as a blastocyst and attaches to the uterine wall.[56] ICM cells are pluripotent, meaning they can differentiate into endoderm-, mesoderm-, or ectoderm-derived cell types but not gametes or placental cells. Induced pluripotent stem cells have equivalent potency to the ICM population and many embryonic stem cell lines are derived from the ICM as well.

Next, several signaling pathways, including Wnt and Nodal, are activated. This causes cells to rearrange and form the primitive streak, a structure on the dorsal side of the embryo that determines body axis patterning. The cells of the primitive streak express the transcription factor Brachyury, a marker of the mesendoderm. An invagination of the endoderm then forms in the blastocyst and cells from the endoderm fill the vacated space and undergo an epithelial-mesenchymal transition to form the mesoderm. This germ layer gives rise to a variety of connective tissues comprising the bones, blood, muscles, and heart.

Brachyury activity then induces expression of the transcription factor Mesoderm Posterior basic helix-loop-helix Transcription Factor 1 (MESP1), a marker for cardiac tissue and adjacent endothelium. MESP1 expressing cell migrate to the anterior side of the embryo and form a structure known as the cardiac crescent. This structure comprises two cell populations: the first and second heart fields. The first heart field gives rise to the left ventricle and part of the atria while the second heart filed gives rise to the right ventricle and the remainder of the atria. MESP1 expression along with inhibition of Wnt signaling initiates expression of several cardiac progenitor markers such as NKX2-5 which is expressed in all cardiac tissue types. The cardiac crescent then forms a primitive

heart tube which contorts and folds over itself to give rise to an adult heart. Retinoic acid signaling activity and expression of markers such as chicken ovalbumin upstream promoter transcription factor 2 (COUP-TFII) lead to atrial formation resulting in a complete four chambered heart.

5.1.5 CRISPR/Cas9 Genome Editing

CRISPR/Cas9 is a powerful tool for performing targeted genome editing and a significant advancement over earlier techniques. It does not require engineering of proteins to bind to the DNA target site like older methods such as Zinc Finger Nucleases or transcription activator-like effector nucleases (TALENS) which makes it cheaper and easier to perform. It is also more versatile because it can target any genomic site with a unique 18-19 base pair arrangement and an NGG DNA base pair sequence where N can represent any base.[35]

To perform CRISPR-mediated genome editing, plasmids encoding the nuclease protein Cas9 and a guide ribonucleic acid (gRNA) with a complementary sequence to the target genomic site are delivered into the cell through viral transduction or transfection. The gRNA then forms a complex with the Cas9 and binds to its complementary target site. The Cas9 then catalyzes a double stranded break of the DNA at the target site. Extensive DNA damage can result in apoptosis but less severe damage is repaired by either non-homologous end joining (NHEJ) or homology direct repair (HDR).

NHEJ is the more common method of repair and is similar to V(D)J recombination used in antibody generation.[57] In this process the protein Ku binds to the broken DNA and serves as a scaffold protein to recruit a variety of proteins such as

kinases and the nuclease Artemis. These proteins then add and phosphorylate nucleotides to make the two ends of DNA compatible. DNA ligase then completes the repair of the deoxyribose backbone. This method often results in changes in the sequence near the break site which can be useful for gene knockouts.[58]

HDR occurs with much less frequency because it relies on the presence of a homologous sequence from a sister chromatid or a transfected donor plasmid to replace the broken DNA. HDR can be used to knock-in new promoters or gene sequences. In this method, a protein complex binds to the broken DNA and chews back both ends to create 3' overhangs. The overhangs are then stabilized by replication protein A (RPA). The protein Rad51 then accumulates as a filament on the 5' end of the DNA opposite the 3' overhang. This filament then recruits the homologous DNA template which is then replicated to complete the break repair.[58]

5.2 Potential Pitfalls and Troubleshooting

It is possible that luciferase will be secreted by only a few of the reporter cells. The reporter cassette, however, also includes GFP; a simple fluorescent image of the cell culture or a flow cytometry experiment would therefore indicate what proportion of the cell population is undergoing marker-induced signaling. High-throughput single cell antibody-based assays capable of detected secreted protein could be employed to characterize heterogeneity within the cell population.[59] There is also a sensitive label free method similar to SPR which can detect secreted markers from single cells in a population.[60]

Design of reporters of transcription factor activity is not trivial. Many reporters have been validated in the literature and adopting these for this application will likely save time and resources. Careful consideration of the design of the enhancer sequences is critical and optimization may be required. The most important parameters to optimize are the spacing and the number of transcription factor binding sequences. Spacing may be informed by crystal structures of the protein of interest if they are available. If not, then related transcription factors could be used to guide the design. The number of repeats of binding sites will have to be optimized experimentally but in general similar reporters use between three and 10 repeats. Cloning repetitive sequences can be difficult because it is hard to find unique sequences for primers to bind to. Therefore it is recommended that enhancer sequences be synthesized and ligated into the existing vector. Based on our experience with the Brachyury reporter, the fold change increases with more repeats but the absolute signal decreases. It is not clear why this is but it may be that too many transcription factors binding at once interferes with the assembly of the transcription complex. Additionally, while some transcription factors known as pioneer transcription factors (e.g., Brachyury) can activate transcription alone, other transcription factors such as NKX2-5 and GATA4 rely on interactions with cofactors which greatly enhance their activity. Another complication to consider is that related transcription factors often target the same DNA binding sites. Specificity of spacing and specific cofactor interactions help mitigate this but care should be taken in the initial design and validation to ensure that the reporters are not being activated non-specifically. Finally, change in cell number over time can alter the baseline signal and make comparing fold changes difficult. To mitigate this issue, characterization of signaling in good and bad differentiations is required to

have a proper standard of comparison. Alternatively, cells could be dual edited with constitutively expressed Cyprindia luciferase, which is also secreted and uses an orthogonal substrate to that of Gaussia luciferase. Gaussia signal could then be normalized to Cyprindia signal for a dual assay.

5.3 Materials and Methods

5.3.1 iPSC Nucleofection

Induced pluripotent stem cells were nucleofected according to a protocol used by Mandegar et al.[61] Briefly, donor plasmid (5 μg), Cas9 plasmid (2 μg), and gRNA plasmid (2 μg) were added to $2*10^6$ dissociated WTC11 iPSCs and nucleofected in an Amaxa nucleofector 2b device using the stem cell nucleofector kit I and program A-23. Cells were then seeded into matrigel coated 6 well plates in mTeSR with Y-27632 an inhibitor of Rho associated protein kinase (ROCK).

5.3.2 CRISPR and Validation of Editing

HEK293T cells or WTC11 iPSCs were transfected with appropriate plasmids as described previously. They were then re-plated into 15 cm diameter culture dishes and allowed to grow to confluence. Upon confluence they were treated with a dose of Puromycin determined using a kill curve. Media was changed daily until only small colonies remain. Colonies were picked via pipette and placed into 96 well plates. These colonies were split and genomic DNA was extracted from a fraction of each colony while the remaining cells propagated the colony. We first validated insertion of the reporter cassette by polymerase chain reaction (PCR) of the extracted DNA with primers that

anneal to genomic DNA near the insert. We then confirmed the location of the insert with PCR in which one primer anneals to the insert and another anneals to the adjacent genome. Positive clones were expanded and frozen stocks made.

5.3.3 Cardiomyocyte Differentiation and iPSC Culture

WTC11 human iPSCs were differentiated into cardiomyocytes based the Allen Institute's modification of the GSK3 inhibition Wnt inhibition (GiWi) protocol[62] developed by Lian et al.[4] Briefly, cells were seeded at 0.3-0.5*10^6 cells in mTeSR1 and 5 μM ROCK inhibitor (ROCKi) in 12 well plates (day -4). For the next three days media was changed to fresh mTESR1 without ROCKi. The next day (day 0) media was exchanged for Roswell Park Memorial Institute with B-27 supplement (RPMI/B-27) without insulin supplemented with 10-15 μM CHIR99021. On day 1 media was replaced with RPMI/B-27 without insulin or CHIR99021. On day 3, old media was combined with new media in a 1:1 volume ratio and IWP-2 was added to a final concentration of 5 μM. On day 5, media was exchanged for new RPMI/B-27 without IWP-2. On day 7 and every three days thereafter media was exchanged to maintain differentiated cells.

5.4 Results

We have developed reporter constructs for the mesodermal marker Brachyury and atrial marker COUP-TFII. The Brachyury reporter consists of 8x Brachyury binding sites followed by a minimal promoter and the firefly luciferase gene. Upon binding to the consensus binding sites, Brachyury initiates the transcription of the luciferase gene without the need for other co-factors. Similarly, the COUP-TFII reporter contains a COUP-TFII responsive promoter and is capable of activating luciferase transcription in

the presence of the maker and endogenous co-factors. These markers were chose because they had been shown to function in HEK293T which makes validation easier. They are also markers of interest in cardiac development.

We cloned these reporter cassettes into the pVitro2 plasmid from Invivogen and validated them with co-transfection of the reporter and the corresponding marker (Figure 17). There was a significant increase in the luciferase response of both reporters in the presence of their respective activator genes.

To validate the efficacy of the iCasp9 suicide gene, HEK293T cells were transiently transfected with the AAVS-1 donor plasmid containing a PGK-iCasp9-T2A-mCherry cassette also used in iPSC genome editing. Confocal microscopy images of the constitutively expressed mCherry in cell populations treated with 0 nM, 0.1 nM, and 10

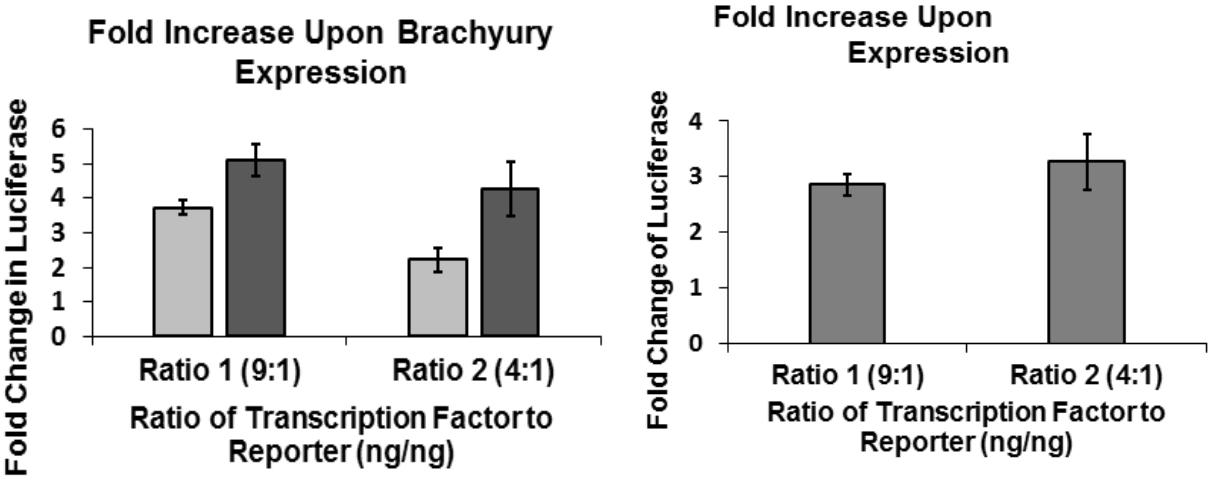

Figure 17 Validation of Brachyury and COUP-TFII Reporter Cassettes A) HEK293T cells were transfected a Brachyury expression vector and Brachyury reporter plasmids with either 4 or 8 consensus binding sequences (light and dark bars respectively) in the indicated mass ratios. Data is reported as a fold change compared to cells transfected with reporter and empty vector. All groups showed significant activation (student's t-test $p < .05$) B) HEK293T cells were similarly transfected with a COUP-TFII expression vector and reporter in the indicated ratios. Both groups showed significant reporter activation compared to the empty vector control (student's t-test $p < .05$)

nM AP1903 suicide inducer molecule for 24 hours show increased puncta formation at higher doses (Figure 18). These puncta are indicative of apoptosis which suggests that iCasp9 suicide gene is effective with AP1903 doses at or above the purported LD50 concentration. The general lack of puncta in the 0 nM control group also suggests that the suicide gene does not reduce cell viability unless the inducer molecule is present (see circled regions).

5.5 Future Work

Cells have been nucleofected to generate reporter lines and a suicide gene line and colonies have survived antibiotic selection. These putatively edited cells will be banked and available for distribution to collaborators shortly. Some characterization will need to be performed including a PCR to indicate on-target editing and a functional assay to ensure the edited lines fulfill their main function. These assays could be done within a few weeks. Functional assays in the case of the reporter lines will include luciferase assays and fluorescent imaging using the GFP channel at the appropriate time in the differentiation protocol. In the case of the suicide gene line, functional assays will comprise a viability assay to characterize cell death after treatment with a range of doses of AP1903 and fluorescent imaging using the RFP channel to show puncta formation indicative of apoptosis.

However, much more thorough characterization would be required before these cells could be employed for in situ monitoring of therapeutic cells during differentiation. Per the Allen Institute for Cell Science, methods of characterization of edited lines should include post thaw viability assays, copy number determination, checking for plasmid

integration or off target mutations with ddPCR, confirming a normal karyotype, assessing the growth rate, characterizing stem cell marker expression, performing germ layer differentiation to ensure pluripotency, performing cardiomyocyte differentiation and characterizing CTnT percentage by flow cytometry, and testing for contaminants like mycoplasma.

5.6 Conclusion

Generation of these reporter cell lines would enable continuous tracking of differentiation of iPSCs through the lengthy and expensive process. Since these luciferase assays would not require lysis and have high sensitivity this would provide feedback which could be used to further improve the culture conditions for differentiation or to abort low quality differentiation attempts prior to completion. For example, these cell lines could enable experiments in which different culture conditions are used and reporter signal is compared between conditions to determine which is best for rapid differentiation of mature cells.

Furthermore these cells could be used to verify the purity of the population. Since these protocols typically result in heterogeneous populations but homogenous populations of ventricular cells are generally desired, the atrial COUP-TFII reporter could provide a sensitive method of detecting undesired cell types.

CHAPTER 6. POTENTIAL FUTURE WORK

6.1 Developing a Fab Heterodimer for Activation of the Non-canonical Wnt Signaling Pathway

In addition to the canonical Wnt pathway discussed extensively throughout this work, there are several other so-called non-canonical Wnt pathways which are of great interest due to their roles in cancer, stem cell differentiation and other processes but are generally less well understood[63]. These include the planar cell polarity (PCP) pathway,

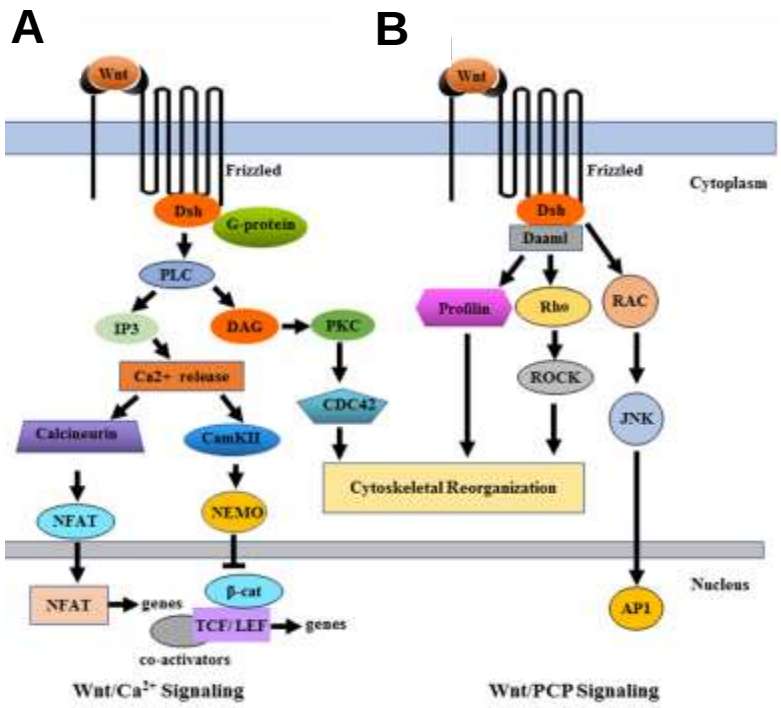

Figure 18. Schematics illustrating A) the non-canonical Wnt calcium pathway and B) the non-canonical Wnt PCP pathway. Figure adapted from Harb et al.[65]

and the calcium pathway as well as other extraneous Wnt-induced signaling events (Figure 18). These non-canonical pathways are initiated by specific Wnt ligands e.g. Wnt-5a, Wnt11, and Wnt4 binding to Frizzled and recruiting receptor tyrosine kinase-like orphan receptor 2 (ROR2) rather than LRP6.[64] In the case of the calcium pathway, this leads to calcium release and transcription of downstream genes regulated by the transcription factors nuclear factor of activated T cells (NFAT) and calcium-dependent protein kinase II (CamKII). In the PCP pathway, Wnt ligands induce gene expression through activation of the transcription factor AP-1[65]. Based on our work with the canonical Wnt agonist, we hypothesize that by analogy a heterodimer consisting of the same anti-Fzd Fab and an anti-ROR2 Fab which targets the same epitope as Wnt-5a would be able to activate one or both of these pathways. Patents containing many antibody sequences exist in the literature[66],[67]. The next requirement for this project is at least one method of verifying non-canonical Wnt signaling. Due to the synergy of CamKII with the Notch pathway[68], the 4×CSL reporter described in Chapter 2 would be suitable for this application.

6.2 Additional Reporter Cell Lines to be Constructed

One of the advantages of the engineered enhancer based reporter approach is that the enhancer sequences can be easily exchanged via vector digestion and gene synthesis of new enhancer sequences. This means, in principle, a reporter could be constructed for almost any transcription factor or group of transcription factors. This versatility combined with the variety of cell types that can be derived from iPSCs means that a reporter could likely be created to track almost any differentiation step in almost any cell type. Cell lines could even be edited at multiple safe harbor sites such as the first intron of CCR5 or the

human analog of the ROSA26 site to permit reporting of multiple phases of differentiation with one line.[69,70]

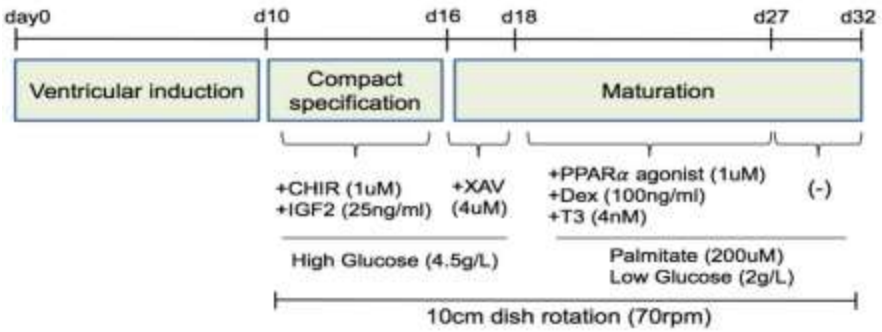

Figure 19. A schematic detailing a protocol for the generation of mature iPSC derived cardiomyocytes. Figure adapted from[71] Funakoshi et al. Nature Comms 2021 with permission https://creativecommons.org/licenses/by/4.0/

An exciting recent work by Funakoshi et al. describes a protocol for making mature ventricular cardiomyocytes[71]. This enables the creation of a variety of reporters for different aspects of maturation which previously could not be validated due to the lack of a positive control for mature iPSC-derived cardiomyocytes (Figure 19). Additional transcription factors of interest that would be beneficial for more robust monitoring of cardiomyocyte differentiation include NKX2-5, HEY2, HIF1α, PGC1α, PPARα, and THRα. NKX2-5 is a very specific marker for cardiac tissue which begins to be expressed during the cardiac progenitor phase. Several enhancer designs which could be used to make an NKX2-5 reporter can be found in the literature[72]. HEY2 is well established marker for mature left ventricular cardiomyocytes used by Funakoshi et al.[71] HIF1α and PGC1α are transcription factors that regulate genes associated with response to hypoxia and lipid metabolism respectively[73],[74]. Oxygen levels control cell proliferation in cardiomyocytes such that hypoxic cardiomyocytes can proliferate but oxygenated

cardiomyocytes cannot. Reduced proliferation is a characteristic of mature cardiomyocytes[73]. Increased lipid metabolism compared to glucose metabolism is also an important characteristic of mature cardiomyocytes[74]. A PPARα agonist and T3 were used by Funakoshi et al as part of their differentiation protocols so reporters of PPARα and THRα which capture these effects would be invaluable. Information gathered by these or similar reporters could be useful in simplifying and optimizing future protocols for differentiation of mature cardiomyocytes.

6.3 A Strategy for Amplifying Reporter Signals in Stable Cell Lines

The reporter constructs discussed in chapter 5 have been validated with transient transfection experiments in HEK293T. These experiments demonstrate that the target transcription factor is capable of binding to the engineered enhancer sequences and capable of producing a detectable signal increase compared to the baseline control. However, this result, while promising, does not guarantee that a reporter validated in this

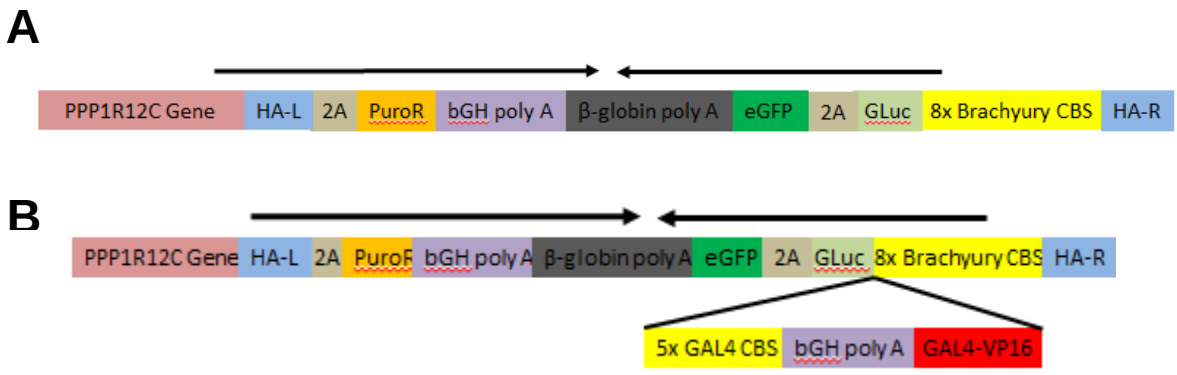

Figure 20. A cartoon illustrating A) A standard one-step reporter cassette and B) A two-step transcription amplification cassette

way will function similarly once integrated into the genome of an iPSC line. This is because the copy number of the reporter will be limited to a maximum of two in genome

edited iPSCs and the expression level of the transcription factor of interest will likely be lower as well. Therefore, a reporter validated in transient transfection experiments may not produce adequate signal in gene edited iPSCs despite the use of highly sensitive luciferases. To ameliorate this issue, we have constructed a two-step transcription amplification (TSTA) system based on the work of Chen et al.[75] (Figure 20). In this system, rather than the transcription factor of interest regulating expression of the reporter genes directly, the protein of interest instead regulates expression of a particularly potent second transcription factor such as a Gal4-VP16 fusion. This second transcription factor then binds to another engineered enhancer site to activate transcription of the reporter gene. This produces a multiplicative signal enhancement, e.g., if the marker of interest alone produces a 2-fold increase in signal, and the secondary transcription factor produces a 4-fold increase in signal, then combined the signal will be boosted 8-fold. Results from preliminary experiments show promise for this approach in our hands (Figure 21).

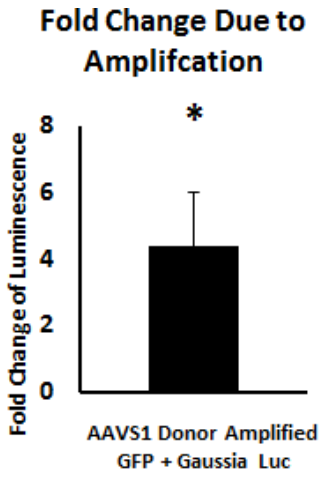

Figure 21. Luciferase assay showing amplification of luminescent signal in TSTA reporter. Data were normalized to the signal from a corresponding non-amplified reporter construct

6.4 Differentiating iPSCs Using Cell Intrinsic Cues

The efficiency of differentiation of iPSCs into cardiomyocytes can reach up to about 80% when using the GiWi protocol previously described[4]. However, even for efficient differentiations, the final cell population is heterogeneous. Rather than a homogenous culture of left ventricular cardiomyocytes, mixed populations containing epicardial cells, endothelial cells, pacemaker cardiomyocytes and atrial cardiomyocytes are typically generated. This heterogeneity is more pronounced at the larger scales needed to produce the more than one billion cardiomyocytes required to treat cardiac damage caused by a typical myocardial infarction. The relationship between scale and heterogeneity can be attributed to differences across different iPSC lines, lot-to-lot

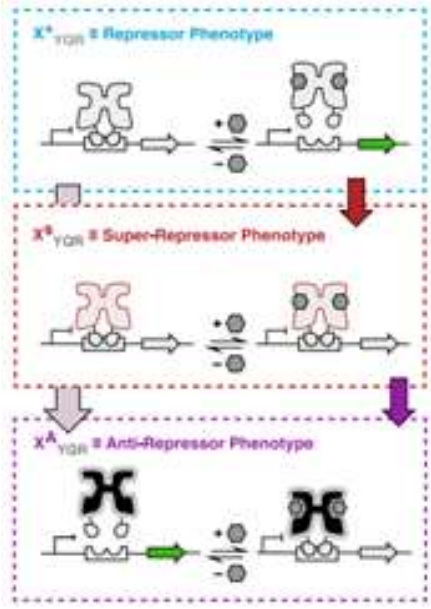

Figure 22. A cartoon illustrating A) A repressor phenotype in which the presence of a ligand induces transcription and B) a super-repressor phenotype in which transcription is repressed regardless of the presence or absence of a ligand C) An anti-repressor phenotype in which transcription is active in the absence of a ligand and is inhibited in the presence of a ligand. Figure adapted from[76] Groseclose et al. Nature Comms 2020 with permission https://creativecommons.org/licenses/by/4.0/

variation in reagents, epigenetic variation in the cell population, and poor control of mechanical and electrical properties in large bioreactors. Engineering cells that can respond to intrinsic differentiation cues rather than extrinsic cues may mitigate these issues.

To accomplish this cell intrinsic control, synthetic biological logic gates could be employed. This approach entails using engineered variants of the Lac operon system or similar operon systems to regulate gene expression.[76,77] These systems consist of naturally occurring bacterial transcription factors which bind to target DNA sequences known as operons. These transcription factors bind to a small molecule ligand which activates or inhibits transcription. For example, in the case of the Lac system, lactose or the synthetic analog IPTG binds to the lac repressor (LacI) to induce transcription of genes associated with lactose metabolism. Making point mutations to the ligand binding domain of the transcription factor can result in changes in phenotype.[76,77] For instance, the Lac repressor can be turned into a super-repressor in which transcription is always off regardless of ligand presence or absence or into an anti-repressor in which transcription is on until the presence of the ligand turns it off (Figure 22). Additionally, point mutations to the DNA binding domain allow targeting to any of seven different operons DNA sequences[76,77].

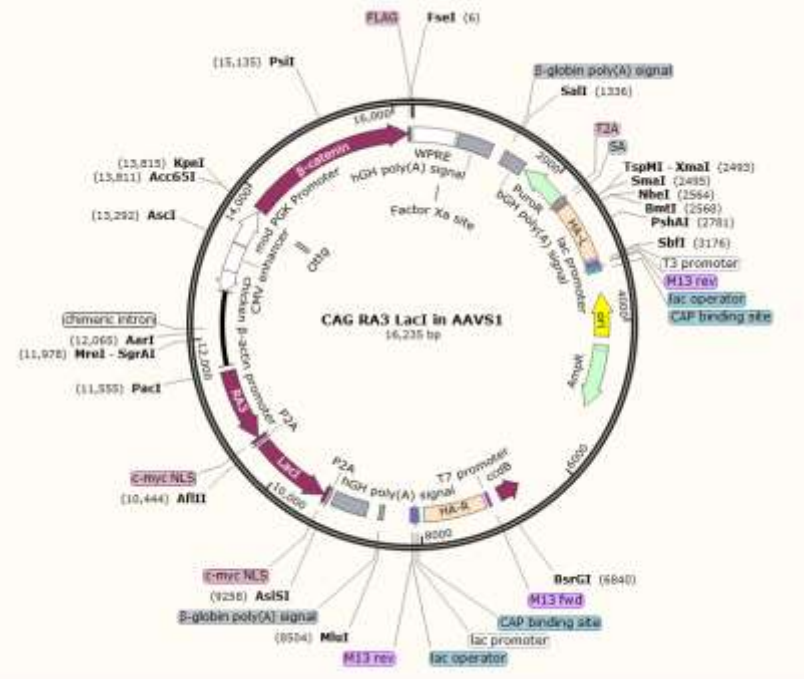

Figure 23. A vector map of a CRISPR donor plasmid which could be used to generate iPSCs lines capable of differentiating into cardiomyocytes in response to cell intrinsic cues

A system of these transcription factors could be used to intrinsically control the Wnt pathway by using operons to regulate transcription of β-catenin. This could be done using the plasmid shown in Figure 24. In this design, the Lac repressor is constitutively expressed and controls expression of β-catenin and the ribose anti-repressor. Thus, when IPTG is added, it induces β-catenin expression and Wnt signaling as well as ribose anti-repressor expression. After some time, the ribose anti-repressor is expressed, binds to the same operon and inhibits β-catenin expression and Wnt signaling in accordance with the GiWi protocol. The timing and extent of the inhibition step will be in proportion to the extent of initial Wnt signaling activation and will follow a timeline determined by cellular processes rather than external cues from the experimenter thus improving differentiation efficiency.

REFERENCES

1. Clevers, H.; Nusse, R., Wnt/beta-Catenin Signaling and Disease. *Cell* **2012,** *149* (6), 1192-1205.

2. Clevers, H., Wnt/beta-catenin signaling in development and disease. *Cell* **2006,** *127* (3), 469-480.

3. Lei, Y.; Schaffer, D. V., A fully defined and scalable 3D culture system for human pluripotent stem cell expansion and differentiation. *Proceedings of the National Academy of Sciences* **2013,** *110* (52), E5039-E5048.

4. Lian, X.; Zhang, J.; Azarin, S. M.; Zhu, K.; Hazeltine, L. B.; Bao, X.; Hsiao, C.; Kamp, T. J.; Palecek, S. P., Directed cardiomyocyte differentiation from human pluripotent stem cells by modulating Wnt/β-catenin signaling under fully defined conditions. *Nature Protocols* **2013,** *8* (1), 162-175.

5. Vazin, T.; Freed, W. J., Human embryonic stem cells: derivation, culture, and differentiation: a review. *Restor Neurol Neurosci* **2010,** *28* (4), 589-603.

6. Takahashi, K.; Yamanaka, S., Induction of Pluripotent Stem Cells from Mouse Embryonic and Adult Fibroblast Cultures by Defined Factors. *Cell* **2006,** *126* (4), 663-676.

7. Mis, M.; O'Brien, S.; Steinhart, Z.; Lin, S.; Hart, T.; Moffat, J.; Angers, S., IPO11 mediates βcatenin nuclear import in a subset of colorectal cancers. *Journal of Cell Biology* **2019,** *219* (2).

8. Nusse, R.; Clevers, H., Wnt/β-Catenin Signaling, Disease, and Emerging Therapeutic Modalities. *Cell* **2017,** *169* (6), 985-999.

9. Janda, C. Y.; Waghray, D.; Levin, A. M.; Thomas, C.; Garcia, K. C., Structural Basis of Wnt Recognition by Frizzled. *Science* **2012,** *337* (6090), 59-64.

10. Willert, K.; Brown, J. D.; Danenberg, E.; Duncan, A. W.; Weissman, I. L.; Reya, T.; Yates, J. R.; Nusse, R., Wnt proteins are lipid-modified and can act as stem cell growth factors. *Nature* **2003,** *423* (6938), 448-452.

11. Nusse, R.; Clevers, H., Wnt/β-Catenin Signaling, Disease, and Emerging Therapeutic Modalities. *Cell* **2017,** *169* (6), 985-999.

12. Gerlach, J. P.; Jordens, I.; Tauriello, D. V. F.; van 't Land-Kuper, I.; Bugter, J. M.; Noordstra, I.; van der Kooij, J.; Low, T. Y.; Pimentel-Muiños, F. X.; Xanthakis, D.; Fenderico, N.; Rabouille, C.; Heck, A. J. R.; Egan, D. A.; Maurice, M. M., TMEM59

potentiates Wnt signaling by promoting signalosome formation. *Proceedings of the National Academy of Sciences* **2018,** *115* (17), E3996-E4005.

13. Davidson, G.; Wu, W.; Shen, J.; Bilic, J.; Fenger, U.; Stannek, P.; Glinka, A.; Niehrs, C., Casein kinase 1 γ couples Wnt receptor activation to cytoplasmic signal transduction. *Nature* **2005,** *438* (7069), 867-872.

14. Mukherjee, A.; Dhar, N.; Stathos, M.; Schaffer, D. V.; Kane, R. S., Understanding How Wnt Influences Destruction Complex Activity and β-Catenin Dynamics. *iScience* **2018,** *6*, 13-21.

15. van de Wetering, M.; Sancho, E.; Verweij, C.; de Lau, W.; Oving, I.; Hurlstone, A.; van der Horn, K.; Batlle, E.; Coudreuse, D.; Haramis, A.-P.; Tjon-Pon-Fong, M.; Moerer, P.; van den Born, M.; Soete, G.; Pals, S.; Eilers, M.; Medema, R.; Clevers, H., The β-Catenin/TCF-4 Complex Imposes a Crypt Progenitor Phenotype on Colorectal Cancer Cells. *Cell* **2002,** *111* (2), 241-250.

16. Paige, S. L.; Osugi, T.; Afanasiev, O. K.; Pabon, L.; Reinecke, H.; Murry, C. E., Endogenous Wnt/β-Catenin Signaling Is Required for Cardiac Differentiation in Human Embryonic Stem Cells. *PLOS ONE* **2010,** *5* (6), e11134.

17. Ueno, S.; Weidinger, G.; Osugi, T.; Kohn, A. D.; Golob, J. L.; Pabon, L.; Reinecke, H.; Moon, R. T.; Murry, C. E., Biphasic role for Wnt/β-catenin signaling in cardiac specification in zebrafish and embryonic stem cells. *Proceedings of the National Academy of Sciences* **2007,** *104* (23), 9685-9690.

18. Marvin, M. J.; Di Rocco, G.; Gardiner, A.; Bush, S. M.; Lassar, A. B., Inhibition of Wnt activity induces heart formation from posterior mesoderm. *Genes & Development* **2001,** *15* (3), 316-327.

19. Naito, A. T.; Shiojima, I.; Akazawa, H.; Hidaka, K.; Morisaki, T.; Kikuchi, A.; Komuro, I., Developmental stage-specific biphasic roles of Wnt/β-catenin signaling in cardiomyogenesis and hematopoiesis. *Proceedings of the National Academy of Sciences* **2006,** *103* (52), 19812-19817.

20. Jiang, Y.; Zhou, Y.; Bao, X.; Chen, C.; Randolph, L. N.; Du, J.; Lian, X. L., An Ultrasensitive Calcium Reporter System via CRISPR-Cas9-Mediated Genome Editing in Human Pluripotent Stem Cells. *iScience* **2018,** *9*, 27-35.

21. Fuerer, C.; Nusse, R., Lentiviral Vectors to Probe and Manipulate the Wnt Signaling Pathway. *Plos One* **2010,** *5* (2).

22. Woolfenden, S.; Zhu, H.; Charest, A., A Cre/LoxP conditional luciferase reporter transgenic mouse for bioluminescence monitoring of tumorigenesis. *genesis* **2009,** *47* (10), 659-666.

23. Li, Y.; Li, S.; Li, Y.; Xia, H.; Mao, Q., Generation of a novel HEK293 luciferase reporter cell line by CRISPR/Cas9-mediated site-specific integration in the genome to

explore the transcriptional regulation of the PGRN gene. *Bioengineered* **2019,** *10* (1), 98-107.

24. Lai, C.; Jiang, X.; Li, X., Development of Luciferase Reporter-Based Cell Assays. *ASSAY and Drug Development Technologies* **2006,** *4* (3), 307-315.

25. Blöchinger, A. K.; Siehler, J.; Wißmiller, K.; Shahryari, A.; Burtscher, I.; Lickert, H., Generation of an INSULIN-H2B-Cherry reporter human iPSC line. *Stem Cell Research* **2020,** *45*, 101797.

26. Chavez, J. C.; Bachmeier, C.; Kharfan-Dabaja, M. A., CAR T-cell therapy for B-cell lymphomas: clinical trial results of available products. *Therapeutic Advances in Hematology* **2019,** *10*, 2040620719841581.

27. Tisoncik, J. R.; Korth, M. J.; Simmons, C. P.; Farrar, J.; Martin, T. R.; Katze, M. G., Into the Eye of the Cytokine Storm. *Microbiology and Molecular Biology Reviews* **2012,** *76* (1), 16-32.

28. Mukherjee, A.; Stathos, M. E.; Varner, C.; Arsiwala, A.; Frey, S.; Hu, Y.; Smalley, D. M.; Schaffer, D. V.; Kane, R. S., One-pot synthesis of heterodimeric agonists that activate the canonical Wnt signaling pathway. *Chemical Communications* **2020,** *56* (25), 3685-3688.

29. Clevers, H.; Nusse, R., Wnt/β-Catenin Signaling and Disease. *Cell* **2012,** *149* (6), 1192-1205.

30. Takada, R.; Satomi, Y.; Kurata, T.; Ueno, N.; Norioka, S.; Kondoh, H.; Takao, T.; Takada, S., Monounsaturated Fatty Acid Modification of Wnt Protein: Its Role in Wnt Secretion. *Developmental Cell* **2006,** *11* (6), 791-801.

31. Chen, E. Y.; DeRan, M. T.; Ignatius, M. S.; Grandinetti, K. B.; Clagg, R.; McCarthy, K. M.; Lobbardi, R. M.; Brockmann, J.; Keller, C.; Wu, X.; Langenau, D. M., Glycogen synthase kinase 3 inhibitors induce the canonical WNT/β-catenin pathway to suppress growth and self-renewal in embryonal rhabdomyosarcoma. *Proc Natl Acad Sci U S A* **2014,** *111* (14), 5349-5354.

32. Roux, M.; Dosseto, A., From direct to indirect lithium targets: a comprehensive review of omics data. *Metallomics* **2017,** *9* (10), 1326-1351.

33. Mukherjee, A.; Dhar, N.; Stathos, M.; Schaffer, D. V.; Kane, R. S., Understanding How Wnt Influences Destruction Complex Activity and beta-Catenin Dynamics. *iScience* **2018,** *6*, 13-21.

34. Maurer, U.; Preiss, F.; Brauns-Schubert, P.; Schlicher, L.; Charvet, C., GSK-3 – at the crossroads of cell death and survival. *Journal of Cell Science* **2014,** *127* (7), 1369-1378.

35. Cong, L.; Ran, F. A.; Cox, D.; Lin, S.; Barretto, R.; Habib, N.; Hsu, P. D.; Wu, X.; Jiang, W.; Marraffini, L. A.; Zhang, F., Multiplex Genome Engineering Using CRISPR/Cas Systems. *Science* **2013,** *339* (6121), 819-823.

36. Janda, C. Y.; Dang, L. T.; You, C.; Chang, J.; de Lau, W.; Zhong, Z. A.; Yan, K. S.; Marecic, O.; Siepe, D.; Li, X.; Moody, J. D.; Williams, B. O.; Clevers, H.; Piehler, J.; Baker, D.; Kuo, C. J.; Garcia, K. C., Surrogate Wnt agonists that phenocopy canonical Wnt and β-catenin signalling. *Nature* **2017,** *545*, 234.

37. Zakeri, B.; Fierer, J. O.; Celik, E.; Chittock, E. C.; Schwarz-Linek, U.; Moy, V. T.; Howarth, M., Peptide tag forming a rapid covalent bond to a protein, through engineering a bacterial adhesin. *Proceedings of the National Academy of Sciences* **2012,** *109* (12), E690-E697.

38. Janda, C. Y.; Dang, L. T.; You, C.; Chang, J.; de Lau, W.; Zhong, Z. A.; Yan, K. S.; Marecic, O.; Siepe, D.; Li, X.; Moody, J. D.; Williams, B. O.; Clevers, H.; Piehler, J.; Baker, D.; Kuo, C. J.; Garcia, K. C., Surrogate Wnt agonists that phenocopy canonical Wnt and β-catenin signalling. *Nature* **2017,** *545* (7653), 234-237.

39. Kane, R. S., Thermodynamics of Multivalent Interactions: Influence of the Linker. *Langmuir* **2010,** *26* (11), 8636-8640.

40. (a) Gurney, A. L. Frizzled-binding agents and uses thereof. US 09499630, Nov 22 2016, 2016; (b) Jenkins, D.; Lei, M.; Loew, A.; Zhou, L. Low density lipoprotein-related protein 6 (LRP6)-half life extender constructs. US 08883735, Nov 11 2014, 2014.

41. Wiśniewski, J. R.; Zougman, A.; Nagaraj, N.; Mann, M., Universal sample preparation method for proteome analysis. *Nature Methods* **2009,** *6* (5), 359-362.

42. Rinker, T. E.; Philbrick, B. D.; Temenoff, J. S., Core-shell microparticles for protein sequestration and controlled release of a protein-laden core. *Acta Biomater* **2017,** *56*, 91-101.

43. Novák, J.; Lemr, K.; Schug, K. A.; Havlíček, V., CycloBranch: De Novo Sequencing of Nonribosomal Peptides from Accurate Product Ion Mass Spectra. *Journal of The American Society for Mass Spectrometry* **2015,** *26* (10), 1780-1786.

44. Mukherjee, A.; Dhar, N.; Stathos, M.; Schaffer, D. V.; Kane, R. S., Understanding How Wnt Influences Destruction Complex Activity and β-Catenin Dynamics. *iScience* **2018,** *6*, 13-21.

45. (a) Azzolin, L.; Panciera, T.; Soligo, S.; Enzo, E.; Bicciato, S.; Dupont, S.; Bresolin, S.; Frasson, C.; Basso, G.; Guzzardo, V.; Fassina, A.; Cordenonsi, M.; Piccolo, S., YAP/TAZ Incorporation in the β-Catenin Destruction Complex Orchestrates the Wnt Response. *Cell* **2014,** *158* (1), 157-170; (b) Hernández, A. R.; Klein, A. M.; Kirschner, M. W., Kinetic Responses of β-Catenin Specify the Sites of Wnt Control. *Science* **2012,** *338* (6112), 1337-1340; (c) Kim, S.-E.; Huang, H.; Zhao, M.; Zhang, X.; Zhang, A.; Semonov, M. V.; MacDonald, B. T.; Zhang, X.; Abreu, J. G.; Peng, L.; He,

X., Wnt Stabilization of β-Catenin Reveals Principles for Morphogen Receptor-Scaffold Assemblies. *Science* **2013,** *340* (6134), 867-870; (d) Li, Vivian S. W.; Ng, Ser S.; Boersema, Paul J.; Low, Teck Y.; Karthaus, Wouter R.; Gerlach, Jan P.; Mohammed, S.; Heck, Albert J. R.; Maurice, Madelon M.; Mahmoudi, T.; Clevers, H., Wnt Signaling through Inhibition of β-Catenin Degradation in an Intact Axin1 Complex. *Cell* **2012,** *149* (6), 1245-1256.

46. Kahn, M., Can we safely target the WNT pathway? *Nature Reviews Drug Discovery* **2014,** *13* (7), 513-532.

47. Mukherjee, A.; Sudrik, C.; Hu, Y.; Arha, M.; Stathos, M.; Baek, J.; Schaffer, D. V.; Kane, R. S., CL6mN: Rationally Designed Optogenetic Photoswitches with Tunable Dissociation Dynamics. *ACS Synthetic Biology* **2020,** *9* (9), 2274-2281.

48. Bugaj, L. J.; Choksi, A. T.; Mesuda, C. K.; Kane, R. S.; Schaffer, D. V., Optogenetic protein clustering and signaling activation in mammalian cells. *Nature Methods* **2013,** *10* (3), 249-252.

49. CDC Heart Disease Facts. https://www.cdc.gov/heartdisease/facts.htm.

50. Alcon, A.; Cagavi Bozkulak, E.; Qyang, Y., Regenerating functional heart tissue for myocardial repair. *Cell Mol Life Sci* **2012,** *69* (16), 2635-2656.

51. Jin, G.; Palecek, S. P., Chapter 6 - Inductive factors for generation of pluripotent stem cell-derived cardiomyocytes. In *Engineering Strategies for Regenerative Medicine*, Fernandes, T. G.; Diogo, M. M.; Cabral, J. M. S., Eds. Academic Press: 2020; pp 177-242.

52. Lian, X.; Zhang, J.; Azarin, S. M.; Zhu, K.; Hazeltine, L. B.; Bao, X.; Hsiao, C.; Kamp, T. J.; Palecek, S. P., Directed cardiomyocyte differentiation from human pluripotent stem cells by modulating Wnt/β-catenin signaling under fully defined conditions. *Nature Protocols* **2012,** *8*, 162.

53. Karakikes, I.; Ameen, M.; Termglinchan, V.; Wu, J. C., Human Induced Pluripotent Stem Cell–Derived Cardiomyocytes. *Circulation Research* **2015,** *117* (1), 80-88.

54. Rangel-Sosa, M.; Aguilar-Córdova, E.; Rojas-Martinez, A., Immunotherapy and gene therapy as novel treatments for cancer. *Colombia Medica* **2017,** *48*, 137-146.

55. Gargett, T.; Brown, M. P., The inducible caspase-9 suicide gene system as a "safety switch" to limit on-target, off-tumor toxicities of chimeric antigen receptor T cells. *Frontiers in Pharmacology* **2014,** *5* (235).

56. Shahbazi, M. N., Mechanisms of human embryo development: from cell fate to tissue shape and back. *Development* **2020,** *147* (14), dev190629.

57. Schatz, D. G.; Ji, Y., Recombination centres and the orchestration of V(D)J recombination. *Nature Reviews Immunology* **2011,** *11* (4), 251-263.

58. Hartlerode, Andrea J.; Scully, R., Mechanisms of double-strand break repair in somatic mammalian cells. *Biochemical Journal* **2009,** *423* (2), 157-168.

59. Lu, Y.; Chen, J. J.; Mu, L.; Xue, Q.; Wu, Y.; Wu, P.-H.; Li, J.; Vortmeyer, A. O.; Miller-Jensen, K.; Wirtz, D.; Fan, R., High-Throughput Secretomic Analysis of Single Cells to Assess Functional Cellular Heterogeneity. *Analytical Chemistry* **2013,** *85* (4), 2548-2556.

60. Juan-Colás, J.; Hitchcock, I. S.; Coles, M.; Johnson, S.; Krauss, T. F., Quantifying single-cell secretion in real time using resonant hyperspectral imaging. *Proceedings of the National Academy of Sciences* **2018,** *115* (52), 13204-13209.

61. Mandegar, Mohammad A.; Huebsch, N.; Frolov, Ekaterina B.; Shin, E.; Truong, A.; Olvera, Michael P.; Chan, Amanda H.; Miyaoka, Y.; Holmes, K.; Spencer, C. I.; Judge, Luke M.; Gordon, David E.; Eskildsen, Tilde V.; Villalta, Jacqueline E.; Horlbeck, Max A.; Gilbert, Luke A.; Krogan, Nevan J.; Sheikh, Søren P.; Weissman, Jonathan S.; Qi, Lei S.; So, P.-L.; Conklin, Bruce R., CRISPR Interference Efficiently Induces Specific and Reversible Gene Silencing in Human iPSCs. *Cell Stem Cell* **2016,** *18* (4), 541-553.

62. Gerbin, K. A.; Grancharova, T.; Donovan-Maiye, R.; Hendershott, M. C.; Brown, J.; Dinh, S. Q.; Gehring, J. L.; Hirano, M.; Johnson, G. R.; Nath, A.; Nelson, A.; Roco, C. M.; Rosenberg, A. B.; Filip Sluzewski, M.; Viana, M. P.; Yan, C.; Zaunbrecher, R. J.; Cordes Metzler, K. R.; Menon, V.; Palecek, S. P.; Seelig, G.; Gaudreault, N.; Knijnenburg, T.; Rafelski, S. M.; Theriot, J. A.; Gunawardane, R. N., Cell states beyond transcriptomics: integrating structural organization and gene expression in hiPSC-derived cardiomyocytes. *bioRxiv* **2020**, 2020.05.26.081083.

63. Komiya, Y.; Habas, R., Wnt signal transduction pathways. *Organogenesis* **2008,** *4* (2), 68-75.

64. Grumolato, L.; Liu, G.; Mong, P.; Mudbhary, R.; Biswas, R.; Arroyave, R.; Vijayakumar, S.; Economides, A. N.; Aaronson, S. A., Canonical and noncanonical Wnts use a common mechanism to activate completely unrelated coreceptors. *Genes & Development* **2010,** *24* (22), 2517-2530.

65. Harb, J.; Lin, P.-J.; Hao, J., Recent Development of Wnt Signaling Pathway Inhibitors for Cancer Therapeutics. *Current Oncology Reports* **2019,** *21* (2), 12.

66. Short, J. M. Anti-ror2 antibodies, antibody fragments, their immunoconjugates and uses thereof. 2017.

67. Liu, C. ROR2 Antibody. 10 March 2016 (10.03.2016), 2016.

68. Ann, E.-J.; Kim, H.-Y.; Seo, M.-S.; Mo, J.-S.; Kim, M.-Y.; Yoon, J.-H.; Ahn, J.-S.; Park, H.-S., Wnt5a Controls Notch1 Signaling through CaMKII-mediated Degradation of the SMRT Corepressor Protein*. *Journal of Biological Chemistry* **2012,** *287* (44), 36814-36829.

69. Pellenz, S.; Phelps, M.; Tang, W.; Hovde, B. T.; Sinit, R. B.; Fu, W.; Li, H.; Chen, E.; Monnat, R. J., Jr., New Human Chromosomal Sites with "Safe Harbor" Potential for Targeted Transgene Insertion. *Hum Gene Ther* **2019,** *30* (7), 814-828.

70. Irion, S.; Luche, H.; Gadue, P.; Fehling, H. J.; Kennedy, M.; Keller, G., Identification and targeting of the ROSA26 locus in human embryonic stem cells. *Nature Biotechnology* **2007,** *25* (12), 1477-1482.

71. Funakoshi, S.; Fernandes, I.; Mastikhina, O.; Wilkinson, D.; Tran, T.; Dhahri, W.; Mazine, A.; Yang, D.; Burnett, B.; Lee, J.; Protze, S.; Bader, G. D.; Nunes, S. S.; Laflamme, M.; Keller, G., Generation of mature compact ventricular cardiomyocytes from human pluripotent stem cells. *Nature Communications* **2021,** *12* (1), 3155.

72. (a) Chen, C. Y.; Schwartz, R. J., Identification of Novel DNA Binding Targets and Regulatory Domains of a Murine Tinman Homeodomain Factor, nkx-2.5(∗). *Journal of Biological Chemistry* **1995,** *270* (26), 15628-15633; (b) Välimäki, M. J.; Tölli, M. A.; Kinnunen, S. M.; Aro, J.; Serpi, R.; Pohjolainen, L.; Talman, V.; Poso, A.; Ruskoaho, H. J., Discovery of Small Molecules Targeting the Synergy of Cardiac Transcription Factors GATA4 and NKX2-5. *Journal of Medicinal Chemistry* **2017,** *60* (18), 7781-7798.

73. Guimarães-Camboa, N.; Stowe, J.; Aneas, I.; Sakabe, N.; Cattaneo, P.; Henderson, L.; Kilberg, Michael S.; Johnson, Randall S.; Chen, J.; McCulloch, Andrew D.; Nobrega, Marcelo A.; Evans, Sylvia M.; Zambon, Alexander C., HIF1α Represses Cell Stress Pathways to Allow Proliferation of Hypoxic Fetal Cardiomyocytes. *Developmental Cell* **2015,** *33* (5), 507-521.

74. Rowe, G. C.; Jiang, A.; Arany, Z.; Kelly, D. P., PGC-1 Coactivators in Cardiac Development and Disease. *Circulation Research* **2010,** *107* (7), 825-838.

75. Chen, I. Y.; Gheysens, O.; Ray, S.; Wang, Q.; Padmanabhan, P.; Paulmurugan, R.; Loening, A. M.; Rodriguez-Porcel, M.; Willmann, J. K.; Sheikh, A. Y.; Nielsen, C. H.; Hoyt, G.; Contag, C. H.; Robbins, R. C.; Biswal, S.; Wu, J. C.; Gambhir, S. S., Indirect imaging of cardiac-specific transgene expression using a bidirectional two-step transcriptional amplification strategy. *Gene Therapy* **2010,** *17* (7), 827-838.

76. Groseclose, T. M.; Rondon, R. E.; Herde, Z. D.; Aldrete, C. A.; Wilson, C. J., Engineered systems of inducible anti-repressors for the next generation of biological programming. *Nature Communications* **2020,** *11* (1), 4440.

77. Rondon, R. E.; Groseclose, T. M.; Short, A. E.; Wilson, C. J., Transcriptional programming using engineered systems of transcription factors and genetic architectures. *Nature Communications* **2019,** *10* (1), 4784.